การเตรียมแผ่นเส้นใยคอมพอสิตพอลิแอนิลีน/พอลิเมทิลเมทาคริเลตสำหรับการรับรู้แอมโมเนีย

นางสาวพิริยา ขวัญพร้อม

วิทยานิพนธ์นี้เป็นส่วนหนึ่งของการศึกษาตามหลักสูตรปริญญาวิทยาศาสตรมหาบัณฑิต
สาขาวิชาปิโตรเคมีและวิทยาศาสตร์พอลิเมอร์
คณะวิทยาศาสตร์ จุฬาลงกรณ์มหาวิทยาลัย
ปีการศึกษา 2555

PREPARATION OF POLYANILINE/POLY(METHYL METHACRYLATE) COMPOSITE FIBROUS MATS FOR AMMONIA SENSING

Miss Piriya Khwanphrom

A Thesis Submitted in Partial Fulfillment of the Requirements
for the Degree of Master of Science Program in Petrochemistry and Polymer Science
Faculty of Science
Chulalongkorn University
Academic Year 2012

Thesis Title	PREPARATION OF POLYANILINE/POLY(METHYL METHACRYLATE) COMPOSITE FIBROUS MATS FOR AMMONIA SENSING
By	Miss Piriya Khwanphrom
Field of Study	Petrochemistry and Polymer Science
Thesis Advisor	Puttaruksa Varanusupakul, Ph.D.

Accepted by the Faculty of Science, Chulalongkorn University in Partial Fulfillment of the Requirements for the Master's Degree

……………………………………... Dean of the Faculty of Science
(Professor Supot Hannongbua, Dr.rer.nat.)

THESIS COMMITTEE

……………………………………..…. Chairman
(Assistant Professor Warinthorn Chavasiri, Ph.D.)

……………………………………... Thesis Advisor
(Puttaruksa Varanusupakul, Ph.D.)

……………………………………..…. Examiner
(Associate Professor Nuanphun Chantarasiri, Ph.D.)

……………………………..….….…. External Examiner
(Nantiya Viriyabanthorn, D.Eng.)

พิริยา ขวัญพร้อม: การเตรียมแผ่นเส้นใยคอมพอสิตพอลิแอนิลีน/พอลิเมทิลเมทาคริเลตสำหรับการรับรู้แอมโมเนีย. (PREPARATION OF POLYANILINE/POLY(METHYL METHACRYLATE) COMPOSITE FIBROUS MATS FOR AMMONIA SENSING) อ.ที่ปรึกษาวิทยานิพนธ์หลัก: อ.ดร.พุทธรักษา วรานุศุภากุล, 66 หน้า.

ในงานวิจัยนี้แผ่นเส้นใยคอมพอสิตพอลิแอนิลีน/พอลิเมทิลเมทาคริเลตได้เตรียมขึ้นด้วยเทคนิคอิเล็กโทรสปินนิงและใช้ในการรับรู้แก๊สแอมโมเนีย ศึกษาปัจจัยในกระบวนการอิเล็กโทรสปินนิง ที่มีผลต่อลักษณะโครงสร้างสัณฐานของเส้นใย โดยวิเคราะห์ด้วยกล้องอิเล็กตรอนแบบส่องกราด พบว่า ขนาดเส้นผ่านศูนย์กลางของเส้นใยอยู่ในช่วง 170-450 นาโนเมตร ตัวทำละลายที่ใช้ในการละลายพอลิเมอร์ส่งผลกระทบต่อทั้งสัณฐานของเส้นใยและขนาดเส้นผ่านศูนย์กลางของเส้นใย ซึ่งเป็นผลจากสมบัติการระเหยและค่าไดอิเล็กทริกของตัวทำละลาย สำหรับศักย์ไฟฟ้า ระยะทางจากเข็มถึงฉากรองรับ และอัตราการไหลของสารละลาย พบว่าส่งผลต่อขนาดของเส้นใยอย่างเดียว ได้ภาวะที่เหมาะสมในการเตรียมแผ่นเส้นใยคอมพอสิตพอลิแอนิลีน/พอลิเมทิลเมทาคริเลต คือ ศักย์ไฟฟ้า 15 กิโลโวลต์ อัตราการไหลของสารละลาย 10 ไมโครลิตรต่อนาที และระยะทางจากหัวเข็มถึงแผ่นรองรับ 10 เซนติเมตร ศึกษาการรับรู้แก๊สแอมโมเนีย โดยตรวจวัดค่าการสะท้อนของแผ่นเส้นใยคอมพอสิตพอลิแอนิลีน/พอลิเมทิลเมทาคริเลตที่ 800 นาโนเมตร ประสิทธิภาพการรับรู้แก๊สแอมโมเนียของแผ่นเส้นใยคอมพอสิตพอลิแอนิลีน/พอลิเมทิลเมทาคริเลตขึ้นอยู่กับตัวทำละลายและปริมาณพอลิแอนิลีนที่ใช้ พบว่าเปอร์เซ็นต์การสะท้อนเริ่มต้น (%R*i*) และการเปลี่ยนแปลงของเปอร์เซ็นต์การสะท้อน (Δ%R) มีค่าเพิ่มขึ้นเมื่อใช้ตัวทำละลายตามลำดับดังนี้ ไดเมทิลฟอร์มาไมด์< ไดเมทิลฟอร์มาไมด์ต่อเอทิลแอซิเทต(1:1)<เอทิลแอซิเทตต่ออะซิโทน (1:1) ส่วนการเพิ่มปริมาณพอลิแอนิลีนทำให้ค่า %R*i* และ Δ%R มีค่าลดลงเมื่อเพิ่มปริมาณของพอลิแอนิลีน นอกจากนี้พบว่าเส้นใยคอมพอสิตพอลิแอนิลีน/พอลิเมทิลเมทาคริเลตที่เตรียมโดยใช้ไดเมทิลฟอร์มาไมด์ต่อเอทิลแอซิเทตอัตราส่วน 1:1 เป็นตัวทำละลาย ให้การรับรู้แก๊สแอมโมเนียได้ดีและเร็วที่สุด โดยมีระยะเวลาของการตอบสนองที่ 7.5 นาที และระยะเวลาของการผันกลับที่ 7.5 นาที

สาขาวิชา ปิโตรเคมีและวิทยาศาสตร์พอลิเมอร์ ลายมือชื่อนิสิต..
ปีการศึกษา 2555 ลายมือชื่อ อ.ที่ปรึกษาวิทยานิพนธ์หลัก..................

5272459923: MAJOR PETROCHEMISTRY AND POLYMER SCIENCE
KEYWORDS: POLYANILINE/ POLY(METHYL METHACRYLATE) / ELECTROSPINNING/ AMMONIA SENSING / COMPOSITE

PIRIYA KHWANPHROM: PREPARATION OF POLYANILINE/ POLY(METHYL METHACRYLATE) COMPOSITE FIBROUS MATS FOR AMMONIA SENSING. ADVISOR: PUTTARUKSA VARANUSUPAKUL, Ph.D., 66 pp.

In this work, polyaniline/poly(methyl methacrylate) (PANI/PMMA) composite fibrous mats were fabricated by electrospinning technique and used as ammonia sensing. Various factors which affect the morphology of fiber were investigated by scanning electron microscopy (SEM). The diameters of obtained fibers were in the range of 170-450 nm. The solvent system used for dissolution the polymer significantly influenced both the fiber formation and diameter of fibers. The main properties of solvents that caused this result are volatility and dielectric constant. The voltage, the distance between a needle and a collector and flow rate of polymer solution only influenced the diameter of the electrospun fibers. The optimum condition for preparation of PANI/PMMA composite fibrous mats was the electric potential of 15 kV, polymer solution flow rate of 10 µL/min and distance between a needle and a collector of 10 cm. In ammonia gas sensing study, the reflectance of PANI/PMMA composite fibrous mats was measured at 800 nm. The sensing performance of PANI/PMMA composite fibrous mats was depended on prepared solvent and %PANI. The initial percent reflection (%R*i*) as well as the change of percent reflection (Δ%R) were increased as a series; DMF < DMF:ethyl acetate (1:1) < ethyl acetate:acetone (1:1). For effect of %PANI, %R*i* and Δ%R was decreased when %PANI increased. Moreover, PANI/PMMA composite fibrous mats using DMF:ethyl acetate (1:1) solvent system gave the best sensing profile and the fastest sensing in which the response time was 7.5 min and recovery time was 7.5 min.

Field of study Petrochemistry and Polymer Science Student's Signature……………………
Academic Year: 2012 Advisor's Signature……………………

ACKNOWLEDGEMENTS

The author thanks many people for kindly providing the knowledge of this study. First, I would like to express my greatest gratitude and sincere thank to my respectful advisor, Dr. Puttaruksa Varanusupakul, for generosity, plentiful instruction, continuous assistance, constructive criticism, inspiration, sincere encouragements, kind enduringness for my mistake, and critical proofreading throughout this research. Additionally, I would like to extend my appreciation to Assistant Professor Dr. Warinthorn Chavasiri, Associate Professor Dr. Nuanphun Chantarasiri and Dr. Nantiya Viriyabanthorn for their valuable suggestions as my thesis committees.

This work cannot be completed without kindness and helps of many people. I would like to thank Dr. Charoenkwan Kraiya, Assistant Professor Dr. Somchai Kiatgamolchai and Dr. Parichatr Vanalabhpatana for suggestion and helpfulness in my research work. I would like to thank Mr. Taweesak Chanduang and Acting Sub Lt. Sira Nitiyanontakit for all their assistance in building all equipments. I also would like to thank Miss Kanchalar Keeratirawee for allowing me to use her instrument in my research and good supports. Furthermore, I would sincere thank to all members of Chromatography and Separation Research Unit (ChSRU) for their helpfulness, kindness, lovely friendship, encouragement and valuable suggestions; especially all members of 1205/1207 Laboratory.

Finally, I would like to thank my beloved family; father, mother, my sister and my intimate friends for all their love, understanding and support.

CONTENTS

Page

Page

LIST OF TABLES

LIST OF FIGURES

Figure **Page**

LIST OF ABBREVIATIONS

cm	Centimeter
nm	Nanometer
°C	Celcius degree
g	Gram
kV	Kilovoltage
M	Molar concentration
min	Minute
sec	Second
mL	Milliliter
µL	Microliter
ppm	Part per million
PANI	Polyaniline
PANI-EB	Polyemeraldine base
PANI-ES	Polyemeraldine salt
PMMA	Poly(methylmathacrylate)
SD	Standard deviation
%w/v	Percentage weight by volume
%w/w	Percentage weight by weight

CHAPTER I

INTRODUCTION

1.1 Motivation of proposer

Ammonia (NH_3) is a highly water-soluble, colorless, irritant gas with a pungent odor and high toxicity, even low concentration level (ppm). It is a natural gas and can also prepare by chemical process. It is widely used in many applications which sometimes both caustic and hazardous. Today, most of the ammonia in the atmosphere is emitted directly or indirectly by human activity. Large quantities of ammonia can be produced from fertilizer production, livestock farming and slurry processing as well as releasing from urines of humans and animals. The worldwide emission of ammonia per year was estimated in 1980 by the European community commission for environment and quality of life to be 20–30 Tg [1].

The maximum limit value for human exposure to ammonia is 25 ppm (18 mg/m^3 of air) for 8 hours and the olfactory limit of detection of ammonia gas is 55 ppm [2]. Ammonia levels below 1 ppm are not expected to cause health problems and most human has a detection threshold of ammonia’s odor at least 1 ppm. Exposure to more concentrated levels (above 25 ppm) for long-term exposure (more than 8 hours) can cause headaches, nausea and intense burning of the eyes, nose, throat and skin. Exposure to very high levels of ammonia gas can cause serious burns to the eyes and lungs and even death. Therefore, detection of ammonia is important. Choice of suitable sensing materials along with efficient microelectronics for the detection system is the key step in such efforts for ammonia [3].

In recent research, there are many principles for measuring ammonia. The well-known measurement is Nessler reaction. The color of Nessler reagent is changed when reacts with ammonia. However, the reagent is considering very toxic. Therefore, ammonia sensing by other methods is developed. Nowadays, the materials such as metal-oxides [4-6], carbon graphites [7-8], organic/inorganic composites [9-10] and conducting polymers [11] as a gas sensor are widely used. Most sensing materials have used metal oxides but there are principal disadvantages of materials and high dependence on the detecting environments. Conducting polymers are alternative materials due to easy processability and fabrication, low poisoning and relatively low cost compared to other materials. Because of their sensitivity at room temperature and their selectivity for specific chemical agents, conducting polymers can use as materials for different types of chemical sensors [11-13]. The measurement of conductivity or optical absorbance of the polymer is performed as the sensor sensitivity. An increase or decrease of bipolaron densities inside the polymer band gap can be occurred due to interaction between the conducting polymer and gas [12].

Among all conducting polymers, polyaniline (PANI) is widely studied because of its high sensitivity, reversible response, shorter response time, ease of synthesis and environmental stability. Base form of PANI is non conductive but it can change into emeraldine salt form which is conductance by doping with some acids such as hydrochloric acid (HCl) and camphorsulfonic acid (CSA). Yuan et al. [13] used HCl doped PANI film for remote detection of ammonia gases by simple optical measurement. The gas vapor induced chemical interactions with the polymer. As a result, the refractive index and optical absorption of the doping polymer changed which made it suitable for the detection of volatile toxic gasses. However, the principle problem of PANI is its low solubility in many common organic solvents and hence difficult to prepare the solution for processing. Therefore, many reports were blending PANI with other polymers such as poly(methyl methacrylate) (PMMA) to improve the mechanical property and processability of PANI in which nanostructure can be formed [14]. Matsuguchi et al. [15] reported that PANI/PMMA blended film showed the high electrical conductivity and good mechanical properties.

Generally, gas sensor can be fabricated by many techniques [2-5, 11]. Casting is conventional process for preparing a thin film. This process has the advantage of simple and easy of operation. Electrospinning is a process for generating fibers with the diameters ranged from nanometers to sub-micrometers. The obtained fibers have high surface area-to-volume ratio and several small pores, which improved an efficiency and sensitivity of gas sensor. Reneker and Chun [16] reported that PANI fibers were successfully formed into a sulfuric acid coagulation bath. However, it is difficult to electrospin PANI as limited by its molecular weight and solubility.

Thus, many reports have electrospinned PANI with other spinnable polymers. Jagadeesh et al. [17] reported the fabrication of PANI blended PMMA by electrospinning technique, which improved electrical properties of PANI. However, commonly solvents used to prepare the polymer blend such as toluene [14-15], N,N-dimethylformamide (DMF) [18-19], *m*-cresol [20-21] and chloroform [22-23] are highly toxic solvent. Therefore, this research was interested in the preparation of electrospun PANI/PMMA composite fibrous mats from the blending solution using low toxicity solvents and used as ammonia gas sensing via optical properties.

1.2 Objective of the research

The objective of this work is to prepare electrospun PANI/PMMA composite fibrous mats and to study various factors which affect the efficiency of composite fibrous mats for ammonia sensing.

1.3 Scopes of the research

1.3.1 Fabrication of PANI/PMMA composite fibrous mats via electrospinning technique from the blending solution in different solvents

1.3.2 Characterization of electrospun PANI/PMMA composite fibers by scanning elcetron microscopy (SEM) and fourier transform infrared spectroscopy (FT-IR)

1.3.3 Investigating the efficiency of PANI/PMMA composite fibrous mats as an ammonia gas sensing material with optical properties

1.3.4 Study the influence of several parameters on the sensor performance such as amount of PANI, and solvent prepared PANI/PMMA solution

1.4 Benefits of the Research

This research aimed to fabric PANI/PMMA composite fibrous mats fabricated by electrospinning technique for ammonia gas sensing.

CHAPTER II

THEORY

2.1 Polyaniline

2.1.1 Properties of Polyaniline

Polyaniline (PANI) was first known in 1835 as “aniline black”, a term used for any product obtained by the oxidation of aniline [24]. PANI is a highly versatile conducting polymer. PANI can be synthesized by chemical oxidation or electrochemical polymerization. The general polymeric structure of PANI is shown in Figure 2.1 containing aniline repeat units connected to form a backbone of alternating nitrogen atoms and benzene rings.

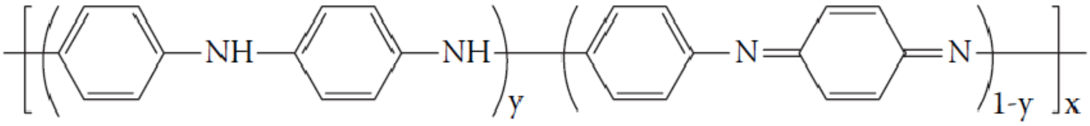

Figure 2.1 The general polymeric structure of PANI [25]

Variety of PANI’s forms differs in chemical and physical properties depending upon the degree of oxidation. Leucoemeraldine with y=1 is the fully reduced state. Pernigraniline is the fully oxidized state (y = 0) with imine links instead of amine links. The emeraldine form that is half oxidized state (y = 0.5) often referred to as emeraldine base (EB) is neutral. This form is the most useful because of high stability at room temperature. When doped with the imine nitrogens protonated by an acid is called emeraldine salt (ES) with the highest conductivity

Table 2.1 The different forms of polyaniline [26]

Form	Name	Color	Conductivity (Scm^{-1})	Structure
Reduced form	Leucoemeraldine base (PANI-LEB)	Yellow, White/clear	$< 10^{-5}$	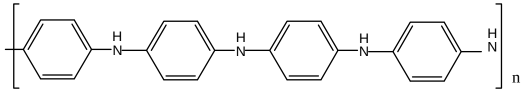
Half oxidized form	Emeraldine base (PANI-EB)	Blue	$< 10^{-5}$	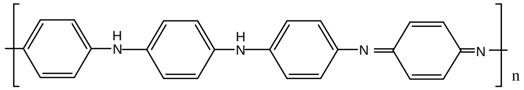
Oxidized form	Pernigraniline base (PANI-PNB).	Blue/Violet	$< 10^{-5}$	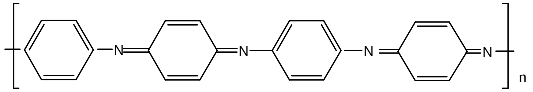
	Emeraldine salt (PANI-ES)	Green	~ 15	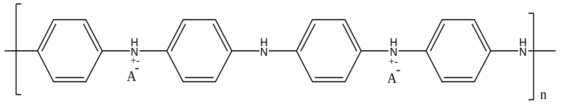

The properties of PANI in different forms are shown in Table 1. In Oxidized form, polyemeraldine salt (PANI-ES) is highest conductivity. Its conductivity is around 15 Scm^{-1} and color is green [27]. Note that the conductivity of a metal is around 10^3 Scm^{-1}. In reduced form, conductivity of polyemeraldine base (PANI-EB) is around 10^{-5} Scm^{-1} and color is yellow or white. Polyaniline can be used in sensor and electrochromic devices because of color change in different oxidation states [28].

2.1.2 Polyaniline synthesis

PANI which is a π-conjugated polymer can be most commonly synthesized through the chemical or electrochemical oxidative polymerization of the respective aniline monomers in acidic solution.

2.1.2.1 Chemical synthesis

For chemical synthesis, three reactants are required to use: aniline, an acidic medium (aqueous or organic) and an oxidant. There are many different oxidants, including: ammonium peroxydisulfate [29-31], hydrogen peroxide [32, 33], ferric chloride [34-36] and cerium sulfate [37, 38]. Acidic conditions ($pH \leq 3$) are usually required to assist the solubility of the aniline in water and to avoid excessive formation of unwanted branched products [39]. The commonly synthesis route is carried out in 1 M hydrochloric acid at pH ~0 and slowly (the reaction is very exothermic) added to each other with an oxidant/aniline molar ratio less than 1.15 in order to obtain high conductivity and yield [40]. The monomer concentration varies from 0.01 to 1 M. The polymerization is executed under 0 to 2 $^{\circ}C$ to avoid secondary reactions. The duration of the reaction is generally between 1 - 2 hours and then polymer precipitates as small particles. The obtained precipitate is PANI-ES: polyemeraldine hydrochloride (PANI-HCl) whose color is green. Polyemeraldine hydrochloride can be converted to polyemeraldine base by deprotonation of the polymer with aqueous ammonium hydroxide.

2.1.2.2 Electrochemical synthesis

Electrochemical polymerization is well-known method to produce PANI without any surfactant and oxidant. The methods can be used galvanostatic method which a constant current is applied ,including potentiostatic method with a constant potential and potentiodynamic method which current and potential are varied with time. A three-electrode system is the best choice to realize synthesis. The components of system are a working electrode which the polymer is deposited, a counter electrode also named auxiliary electrode (platinum grid) and a reference electrode (in most cases, a saturated calomel electrode (SCE)). Working electrodes produced from various materials have been successfully utilized in depositing conducting polymers, such as gold, platinum, and stainless steel [11]. Deposition of PANI have been achieve onto conducting glass (glass covered by indium-doped tin oxide (ITO) electrode), stainless steel, graphite, Fe, Cu, Au, etc [41]. PANI can be easily peeled off from the electrode surface due to carried out in an acidic aqueous solution. Electrochemical synthesis exhibits several advantages [42] such as synthesis and deposition of PANI thin layer can be simultaneously occurs, cleanliness because of no extraction from the monomer solvent-oxidant mixture, doping and thickness can be controlled via electrode potential.

Bhadra et al. [43] compared between chemical synthesis and electrochemical synthesis. They found that the electrochemical synthesis has quite lower conductivity, higher solubility, more benzenoid rings than quinoid rings, lower crystallinity, higher band energy, and higher particle size than the chemical synthesis.

2.1.3 Polyaniline doping

The conductive properties of PANI arise from the doping process. The doping process is a charge-transfer reaction between an organic polymer and a dopant. There are two different pathways in the doping processes; a dopant accepting charges (p-type) or donating charges (n-type) onto the polymer backbone. Conducting mechanism of PANI induces either by the oxidation of the polyleucoemeraldine base or by the protonation of the polyemeraldine base. The two pathways are shown in Figure 2.2.

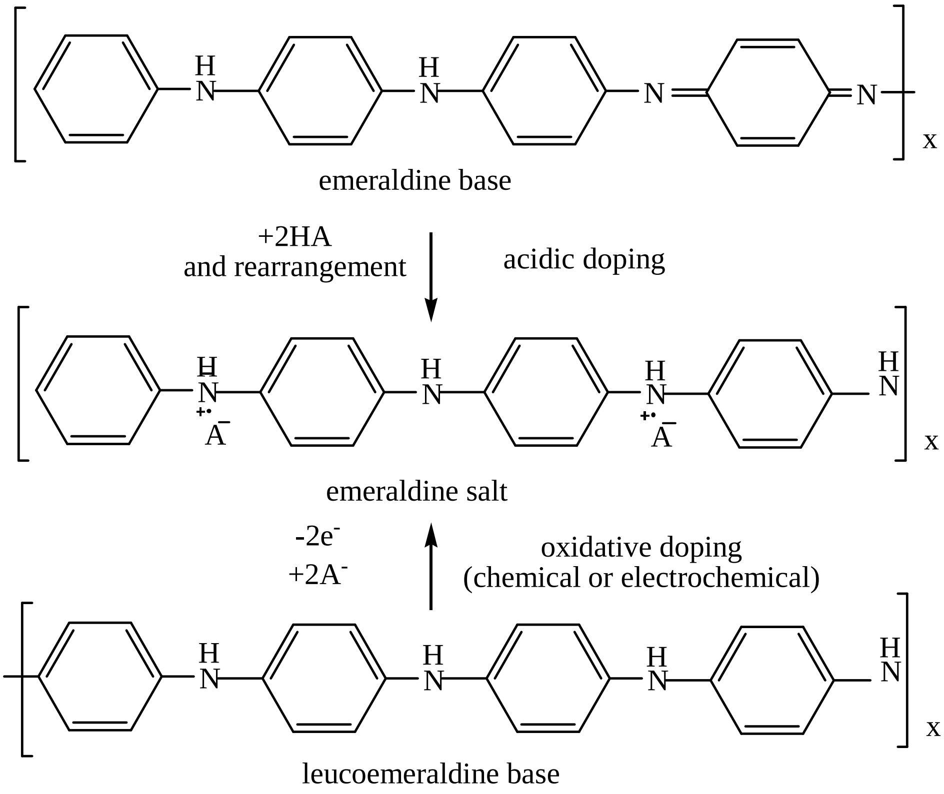

Figure 2.2 Doping mechanisms of PANI [44]

2.1.3.1 Oxidative doping

Chemical or electrochemical process of polyleucoemeraldine base (PANI-LEB) is called oxidative doping. PANI-LEB was prepared by reduction of PANI-ES with phenylhydrazine or hydrazine solutions [45]. The chemical oxidative doping can run through three processes; a chlorine or a less toxic iodine agents in a carbontetrachloride solution, $(NO)^+(PO_6)^-$, $FeCl_3$ or $SnCl_4$ in organic solution, oxygen or hydrogen peroxide in an aqueous acid solution. The following examples illustrate the oxidative doping with Cl_2:

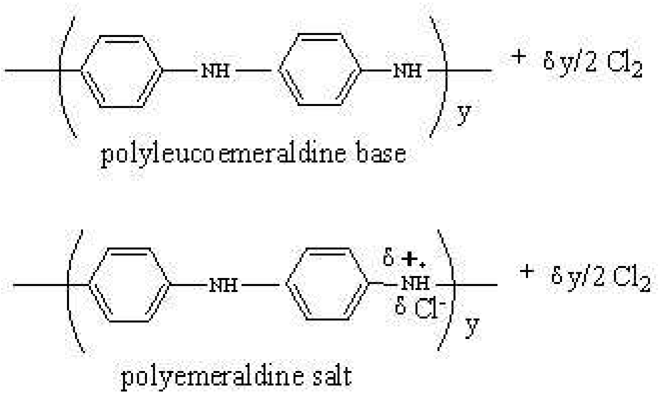

With H_2O_2 in an acidic solution HA:

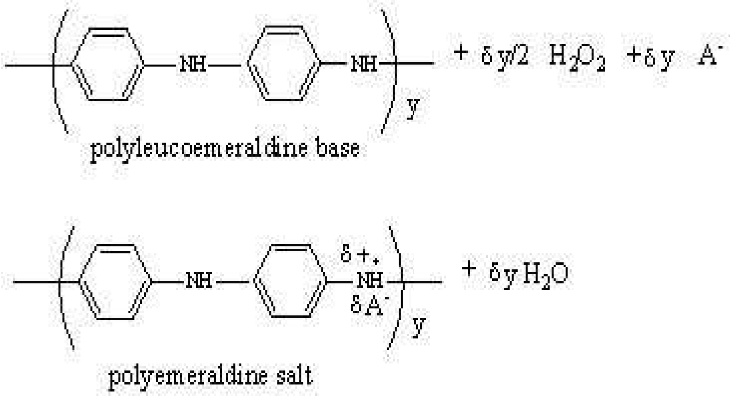

In the latter instance, the nature of the counter-ion A^- (Cl^-, HSO_4^-, $H_2PO_4^-$) is controlled. When Cl_2 is considered both as the oxidant and the dopant, H_2O_2 only oxidizes PANI doped with the acidic solution. Chemical oxidative doping is an easy and efficient process but the control of the doping level (δ) is difficult. This problem can be solved by electrochemical oxidative doping since the doping level is defined by the electric potential applied between the conducting polymer and the counter electrode [46]. PANI-LEB's electrochemical doping can be illustrated as:

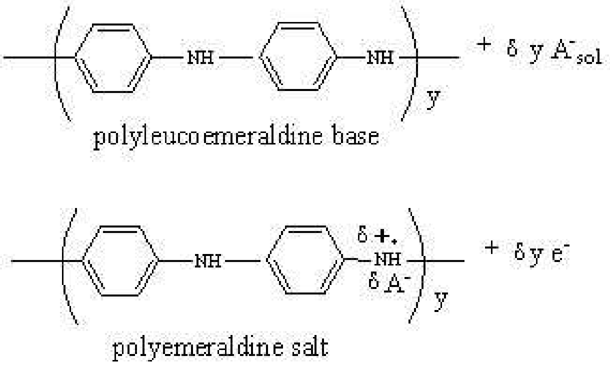

2.1.3.2 Acidic doping

Acidic doping/dedoping mechanism is known through protonation and deprotonation process of PANI with a change in the conductivity and in the color. The acidic doping process is no change of the number of electrons associated with the polymer backbone. Generally, HA type acid (such as HCl, H_2SO_4) has been used to produce conductivity PANI. In solution, the acid can be dissociated into proton (H^+) and acid radical (A^-). Receiving protons of neutral PANI molecules are obtained forming energetically favourable N^+-H chemical bonds. Thus, positively charged local centres placed at nitrogen atoms are formed. The conductivity can be arised from hopping of valence electons from one such centre to another [47]. Acidic doping mechanism can be described that the imine sites, which contain in PANI-EB, was protonated to achieve the intermediate bipolaron form and then dissociated to polaron form. The stage of mechanism is shown in Figure 2.3. The charge carriers responsible for the high conductivity of PANI are poralon form [48]. For the resonant structures, the delocalization of charge and spin can be that explains the conductivity of PANI. Wan and Yang [49] reported that the overall conduction occurs both across and along the chain. The former is depended on the extent of π-electron conjugation along the chain whereas the latter is depended on the transport of charge carriers across the inter chain.

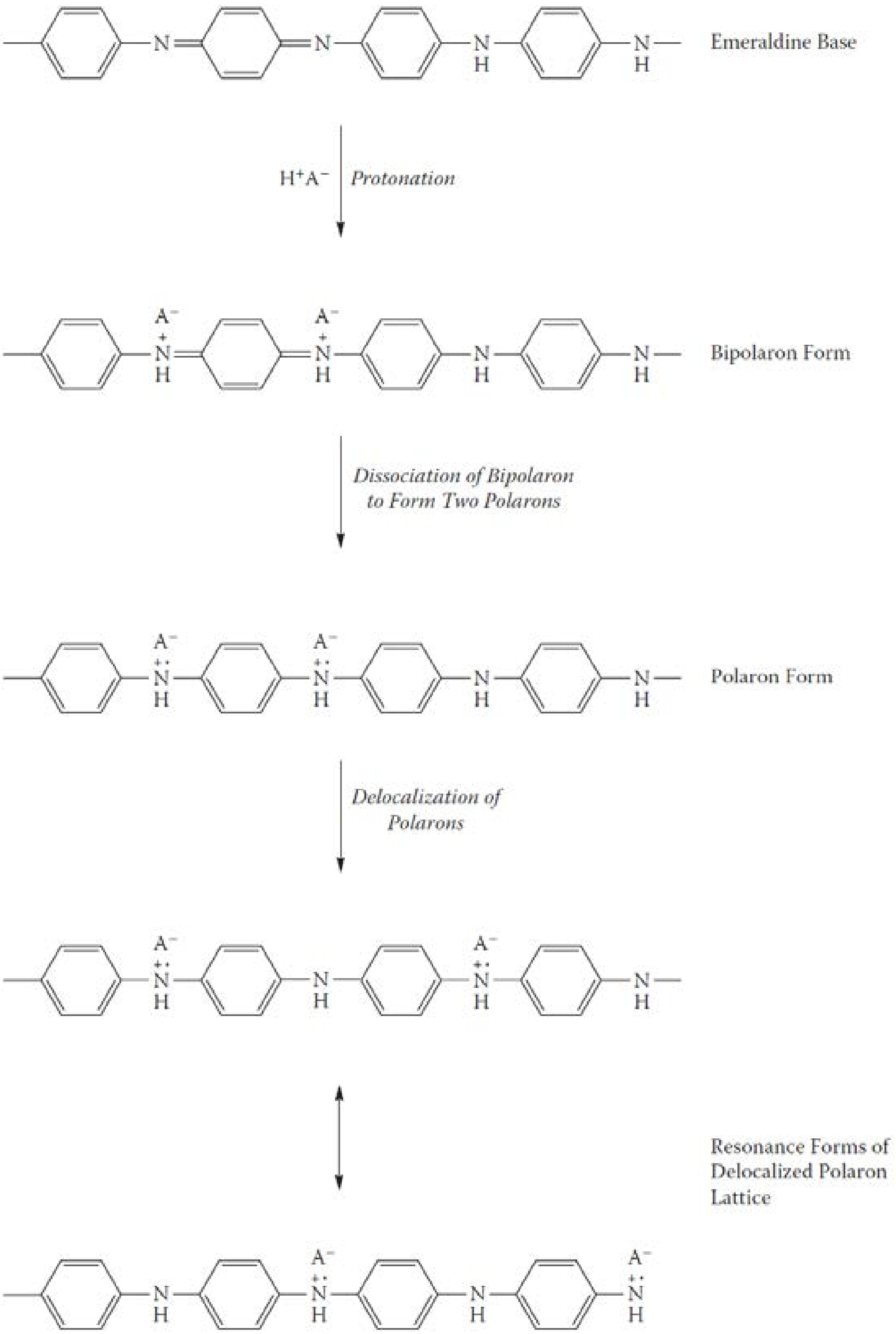

Figure 2.3 The stage of acidic doping mechanism [48]

However, disadvantages of hydrochloride PANI-ES are its conductivity related to moisture and temperature, and its poor solubility in most common solvents. So, polyacrylic acid [50] or other polymeric acids, acrylic acid (AA) [51], lithium salts [50] and voluminous acids, specially sulfonic acids with a long backbone as dodecylbenzensulfonic acid (DBSA) or camphorsulfonic acid (CSA) were used to enhance this problem by added as dopants in the monomer solution [52]. The different dopant results in distinct responses to a specific analyte.

2.2 Ammonia sensing of PANI

Generally, conducting polymer gas sensor depends on conductivity changes that occur when they are exposed to certain gas. Not only conductivity but also optical property can be used for gas sensor due to many different oxidation states of PANI as shown in Table 2.1. The type of dopant affects the mechanism of ammonia sensing, which mineral acid HA (A = Cl^-, HSO_4^-, ClO_4^-) are most often used that call PANI doping (protonation). When ammonia gas is adsorbed on surface of PANI-ES, it interacts with the NH groups of PANI-ES and takes proton to form the NH_4^+ groups. Thus, PANI-ES can be reduced to PANI-EB, resulting in significant changes in electrical conductivity and electronic absorption spectrum. This property of polyaniline has been utilized for developing chemical sensors, especially gas sensors [53-57]. This reaction calls PANI dedoping (deprotonation). In the air (with no ammonia replenishment), ammonium decomposes into ammonia (ammonia volatile-zation) and proton which being added to PANI-EB and restore the initial level of doping PANI-ES as shown in Figure 2.4.

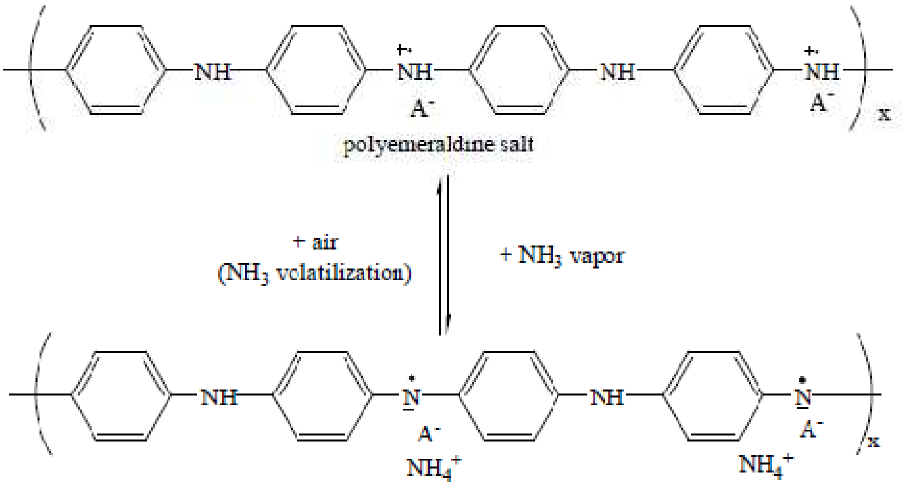

Figure 2.4 Interpretation of the sensitivity and reversibility of PANI-HA layer [58]

2.3 Diffuse reflection

The optical phenomenons are absorbance, fluorescence and reflectance. They can be measured the changing optical property of optical sensor. The optical sensor is a device that consists of the specific perception area and the transducer that converts the recognition process into measurable optical signal properties [59].

Generally, diffuse reflectance which is one type of optical phenomenons is used in the UV-visible, near-infrared and mid-infrared regions. A reflectance spectrum is obtained by the collection and analysis of surface-reflected electromagnetic radiation as a function of frequency (ν usually in wavenumbers, cm^{-1}). The reflection of light can be roughly categorized into two types of reflection: specular reflection is defined as light reflected from a smooth surface at a definite angle, and diffuse reflection, which is produced by rough surfaces that tend to reflect light in all directions as shown in Figure 2.5. Normally, diffuse reflection can occur more than specular reflection.

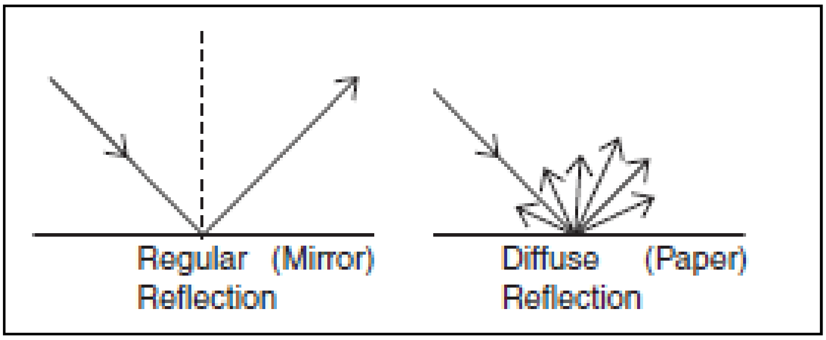

Figure 2.5 The pattern of regular and diffuse reflection [59]

The Kubelka-Munk theory [60, 61] is often used to describe and contemplate diffuse reflectance. The Kubelka-Munk (*F(R)*) is defined as:

$$F(R) = \frac{(1-R)^2}{2R}$$

Where *R* is percent reflectance measured with respect to a standard white. *F(R)* can be related to concentration of analyte by [60].

$$F(R) = \frac{2.303\varepsilon C}{s}$$

Where *ε* is absorbtivity, *C* is the concentration of analyte and *s* is the scattering coefficient of sample surface. By assuming the absorbtivity and scattering coefficient of surface are constant at a given wavelength, Thus, *F(R)* can be related directly to analyte concentration.

2.4 Electrospinning

2.4.1 Basic set-up and mechanism of electrospinning process

Electrospinning is a straightforward, low cost and unique method to produce novel fibers with the diameters ranged from nanometers to sub-micrometers. In 1934, the process was patented by Formhals [62]. The obtained fibers have high surface area-to-volume ratio and several small pores. There are varieties of applications for the fibers including tissue scaffolding, highly efficient filtration membranes, nanowires, nanocomposites, electrical and optical sensors, electrode materials, protective clothing, biomedical, pharmaceutical and catalyst, etc. The electrospinning process uses electrostatic force as the main driving force for fiber formation from melt polymer or polymer solution. The basic set-up consists of three major components including

- a high voltage power supply with positive or negative polarity
- a spinneret such as pipette tip, a capillary with metal needle
- a collector such as a metal screen, stationary plate, and rotation drum or mandrel

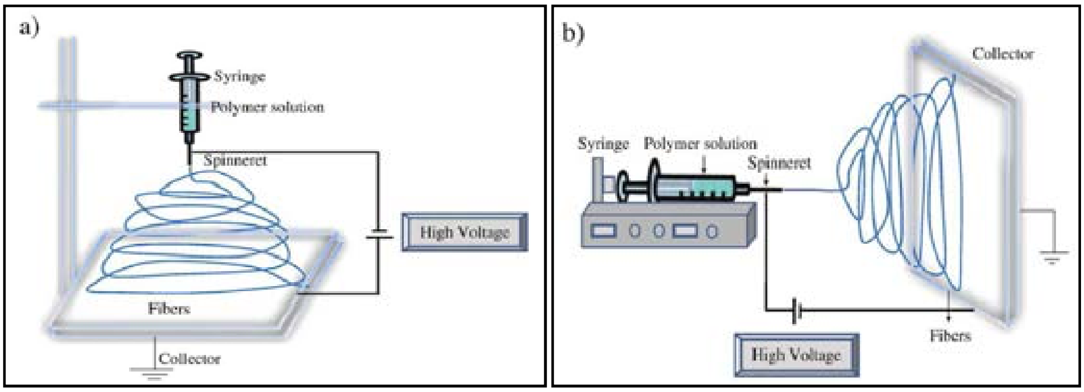

Figure 2.6 Schematics of set-up of electrospinning apparatus [63]:
(a) a typical vertical set-up, (b) a typical horizontal set-up

Figure 2.6 shows two typical experimental set-ups for electrospinning including a vertical and a horizontal apparatus. In the electrospinning process, a high voltage is used to produce an electrically charged jet of polymer solution or polymer melt out of spinneret. One electrode is placed into the spinning polymer solution and the other attached to a collector. Electric field is subjected to the end of a capillary that contains the polymer fluid held by its surface tension. When electric force was increased, the solution at end of capillary will change its shape from semicircle to conical form well-known as “Taylor cone”. When the critical voltage is exceeded, the electrical force overcomes the surface tension and a fine charged jet is unstable causing the extension of jet, reduction of diameter. In the meantime, organic solvent was evaporated as seen in Figure 2.7.

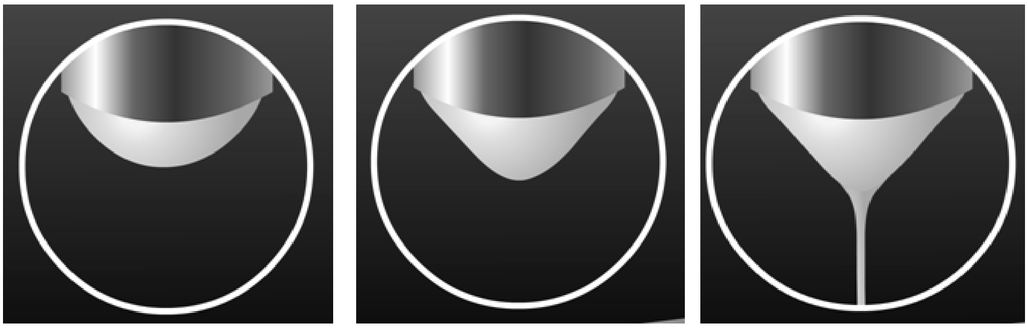

State I **State II** **State III**

Figure 2.7 The model of polymer solution changing when electric potential increases [64]

2.4.2 Parameters of electrospinning process

The variables that affect morphology and properties of electrospun fibers can be divided into two groups. First group is the materials variables relating to polymer and solvent characteristics such as the surface tension, the viscosity, the concentration of the solutions and molecular weights. Another group is the process variables involving equipments and operating parameters such as electric potential, distance between needle and collection screen, and flow rate of solution. The description those are classified as shown in Figure 2.8.

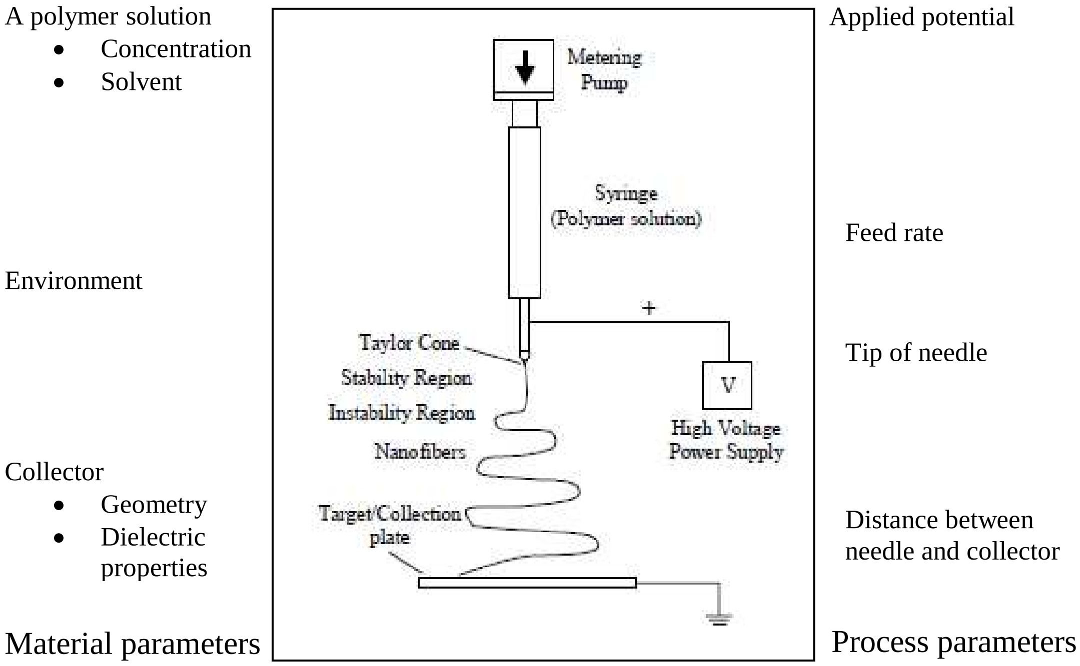

Figure 2.8 The basic materials and process variables in electrospinning of polymer nanofibers [65]

2.4.2.1 Solution parameters of electrospinning

2.4.2.1.1 Concentration

The concentration, molecular weight of polymer and viscosity are related to each other that if used high molecular weight is effect to high concentration and high viscosity. The concentration or viscosity allowing adequate chain entanglement, continuous uniform fibers can be electrospun from polymer solution in a strong enough electric field and also affects much on the diameter of fibers. The diameter and the appearance of electrospun fibers are resulted from the concentration or viscosity of solution. At high concentration, beads can convert from globular to pivot form and a fiber with larger diameters is created because of the increasing of viscosity resistance within solution and the inability to uphold the solution flow at the end of the needle tip. At low concentration, both beads and the fibers are formed [66].

Deitzel et al. [67] studied the concentration range of 4−10 wt% of PEO/water solution. At the low concentration, the result showed an irregular, undulating morphology with large variation in diameter along a single fiber. At the high concentration, the fibers are regular, larger diameter and more uniform.

Afifi et al. [68] reported effect of polymer molecular weight on the electrospinning of polylactides (PLA). At low molecular weight of used polymer (low viscosity) resulted in formation of beads or beads-on-strings, while high viscosity gave homogeneous fibers at optimum conditions.

2.4.2.1.2 Solvent system

The principle of solvent selection is determined by [65] conformation of the dissolved polymer chains, ease of charging the spinning jet, cohesion of the solution due to surface tension forces and rate of solidification of the jet on evaporation of the solvent. Thus, solvent is important role that affected to morphological appearance and electrical resistance.

2.4.2.1.3 Surface tension

Surface tension is important role parameter in the electrospinning process. Normally, the high surface tension of solution forbids the process of spinning due to an unsteadiness of the jet and the production of sprayed droplets [69, 70]. Bead formation in electrospinning can be induced by changing the surface tension of the solution [71]. Whereas the lower surface tension of solution is not always suitable for electrospinning, but the obtained electrospun fibers from this has no bead formation. Surface tension of polymer solutions changes with concentration [67] as well as with the chemical nature of the polymer [72].

Shawon and Sung [73] studied the effect of electrostatic voltage, viscosity and surface tension on electrospun polycarbonate nanofibers with solvent mixtures THF and DMF. They reported that the formation of beads and beaded fibers was driven by the surface tension which depended on polymer and solvent. During the electrospinning of polycarbonate with increased THF and DMF ratios, the solution was noticed to lose the capability to form more fibers than bead due to higher THF evaporation rate. It was expected that surface tension of the higher THF/DMF solutions gradually increased and therefore the solution lost the capability to form more fibers against the relatively higher surface tension.

2.4.2.1.4 Dielectric constant

The dielectric constant is a constant that indicates how easy a material can be polarized by imposition of an electric field on an insulating material at any temperature. The interacted differently of electric field is affected by solvent with different values of dielectric constant. Furthermore, this parameter is effect on the morphology and diameter of electrospun fibers.

Dong et al. [74] studied the effect of molecular weight, solution concentration, solvent dielectric constant, and addition of soluble organic salts. In particular, the dielectric constant was most examined.They reported that high dielectric constant solvents dramatically reduce both the bead formation and diameter of the fibers.

2.4.2.2 Processing parameters of electrospinning

2.4.2.2.1 Electric potential

One of the main roles that affect to morphology and diameter of fibers is electric potential or voltage to polymer solution. When increasing electric potential, the electrostatic repulsive force on the polymer jet is increased. As a result, the fiber diameter is decreased. The effects of electric potential on morphology and diameter of fiber have to be considered concurrently with other parameters, particularly the flow rate and the distance between the needle and the collection screen [66].

2.4.2.2.2 Distance between a needle and a collector

The distance from needle to collector has an influence on the time available for evaporation of the solvent (flight time) and the strength of the electric field. Chowdhury and Stylios [75] reported that the collected fibers are dried, completely stretched, and the fiber diameter is reduced when increased the distance from needle to collector. Therefore, solvent evaporation requires optimum distance between a tip and collector.

2.4.2.2.3 Diameter of needle

The diameter of needle affects the characteristic of fibers. The bead and clogging formation are abated with a small needle diameter. The surface tension of the droplet is increased when the size of the droplet is decreased. Thus, the acceleration of jet decreases, and this allows more time for the solution to be stretched and elongated before it was collected. Nonetheless, if the used needle diameter is too small, it cannot be ejected a droplet of solution. Mo et al. [76] studied the effect of diameter of needle that found the changing diameter of fiber. In other words, the clogging and the amount of bead were found when used large needle diameter. On the other hand, the diameter of fiber was reduced when used a small needle diameter.

2.4.2.2.4 Flow rate of solution

Flow rate can influence the velocity of the jet fluid, solvent evaporation and morphology of the fibers. At low flow rate, the obtained fibers are fine and no bead form due to enough time for solvent evaporation. Rodoplu and Mutlu [77] studied the effects of electrospinning set-up and process parameters. They found that the bead size was decreased till no bead when flow rate was decreased. As a result of further decreased flow rate, it was the necessity of an increase in voltage in order for the electrospinning to take place. Moreover, the characterization of used low flow rate fibers was smooth and fine fiber.

However, the important parameters including electric potential, flow rate, concentration and distance tip to collector affect on the diameter of fibers as shown in Figure 2.9.

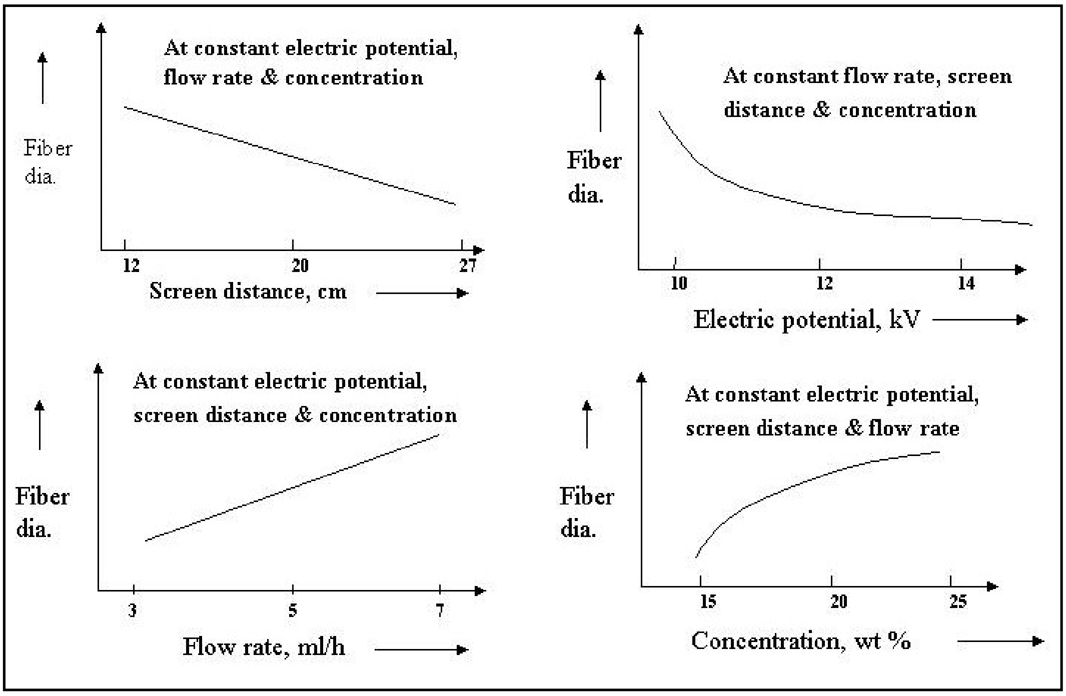

Figure 2.9 Effect of parameters on fiber diameter [78]

CHAPTER III

EXPERIMENTAL

3.1 Materials

1) Polyaniline (PANI; MW 65,000) (Sigma Aldrich, Germany)
2) Poly(methyl methacrylate) (PMMA; MW 350,000) (Sigma Aldrich, Germany)
3) Camphorsulfonic acid (CSA) 99% (Sigma Aldrich, Germany)
4) Ethyl acetate (Merck, Germany)
5) Acetone (Merck, Germany)
6) N,N-dimethylformamide (DMF) (Riedel-de Haën, Germany)
7) 1-Methyl-2-pyrrolidone (NMP) (Fluka, USA)

3.2 Methodology

3.2.1 Preparation of PANI/PMMA solution

1% (w/v) PANI solution was prepared by dissolved 0.05 g of PANI in 5 mL of NMP and stirred for 1 hour at room temperature. Any particulate matter was removed by filtration with 0.45 μm polytetrafluoroethylene (PTFE) filter. PANI was doped with CSA by adding 0.08 g of CSA into PANI solution and stirred for 1 hour. Different volume of PANI was used in each condition of electrospun PANI/PMMA fibers (Table 3.1).

6% (w/v) PMMA was prepared by dissolved PMMA in solvent system including DMF, DMF:ethyl acetate (1:1) and ethyl acetate:acetone (1:1) composition stirred and heated at 50 ^{o}C.

PANI/PMMA solutions at different compositions as in Table 3.1 were prepared by mixing PANI solution with PMMA solution and stirred for 1 hour.

Table 3.1 Composition of PANI/PMMA solutions for fabricating electrospun PANI/PMMA fibrous mats

condition	PMMA solution		PANI solution	PANI/PMMA fibers	
	PMMA (g)	**Solvent (mL)**	**1% (w/v) PANI (mL)**	**PMMA (%w/w) [a]**	**PANI (%w/w) [a]**
1	0.30	5.00	1.00	96.8	3.2
2	0.30	5.00	0.75	97.6	2.4
3	0.30	5.00	0.50	98.4	1.6
4	0.30	5.00	0.25	99.2	0.8

[a] a percentage by weight of PMMA or PANI in PANI/PMMA fibers

3.2.2 Fabrication of PANI/PMMA fibers by electrospinning

An apparatus of electrospinning process (Figure 3.1) consists of high voltage power supply (230 series, Bertan High Voltage Research), syringe pump (NE-1000, Prosense) and collector. The collector is simply a copper plate covered with aluminum foil and connected to ground. The PANI/PMMA solution was filled in syringe bearing a 20G needle, which was connected to high voltage power supply and controlled the flow of solution by syringe pump. The electrospinning condition was varied as follow; the electric potential of 10, 15 and 20 kV, the distance between the needle tip and collector (*d*) of 5, 10 and 15 cm and the flow rate of the solution at 10 and 15 µL/min. Subsequently, the aluminum foil was removed from the collector, and dried in an oven at 80 °C for 6 hours.

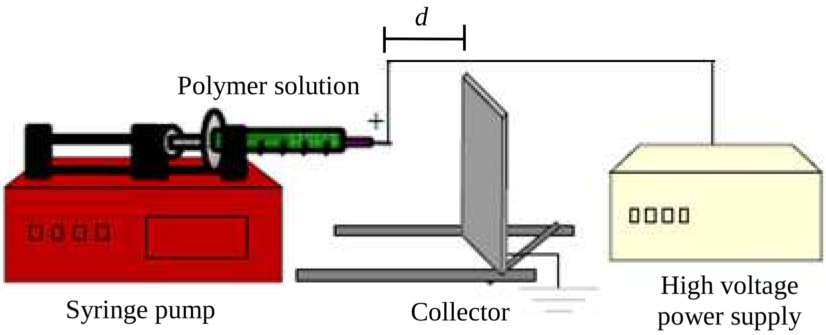

Figure 3.1 Schematic set-up of the electrospinning process

3.2.3 Characterization of electrospun fibers

3.2.3.1 Fourier transform infrared spectrometry (FT-IR)

FT-IR was used to identify the characteristic functional groups of PANI-EB and PANI-ES powders and the fiber mats of PMMA and PANI/PMMA. Infrared spectra were recorded by KBr technique using a FT-IR spectrometer (Nicolet 6700, U.S.A.) at the wavenumber range of 400-4000 cm^{-1} using the transmittance mode with 32 scans and the wavenumber resolution of ±4 cm^{-1}.

3.2.3.2 Scanning electron microscopy (SEM)

The morphology of the electrospun fibers was determined using JEOL scanning electron microscope (SEM; model JSM-5410 LV, Japan). The diameter of fibers was reported as the average values with standard deviation (n=30) by Image Tool 3.0 software (Shareware provided by UTHSCSA).

3.2.3.3 Reflection spectroscopy

The color and optical properties change of PANI-EB and PANI-ES were investigated by measurement of reflection. The PANI-EB was prepared by treated PANI-ES with 6 M of NH_3 at room temperature for 2 hours. The spectra of PMMA, PANI-EB and PANI-ES were monitored with scan wavelength mode by fiber-optic spectrophotometer (Aventes BV, Netherlands). The set-up of reflection measurement was shown in Figure 3.2.

3.3 Ammonia sensing

3.3.1 Experiment set-up for ammonia sensing

The optical properties change was observed by reflectance measurement which apparatus consists of fiber-optic spectrophotometer (Aventes BV, Netherlands). The concentration of ammonia gas used in this system was 1000 ppm balanced with N_2 (TIG, Thailand). The reflectance was measured under dark condition in order to reduce any interference from ambient light. The apparatus for ammonia sensing was shown in Figure 3.2. The chamber was made from black acrylic resin except the top window was clear acrylic resin. The sample on glass watch was inserted in a chamber and then ammonia gas was released through the gas in line. A flow rate of 10 mL/min was controlled by valve and flow meter 1. The response of PANI/PMMA composite fibrous mats were observed by flowing ammonia gas for 10 min. The recovery of PANI/PMMA composite fibrous mats were observed by purging the chamber with nitrogen gas at a flow rate of 10 mL/min controlled by vale and flow meter 2. The reflectance of PANI/PMMA composite fibrous mats was detected and recorded every second via fiber-optic spectrophotometer.

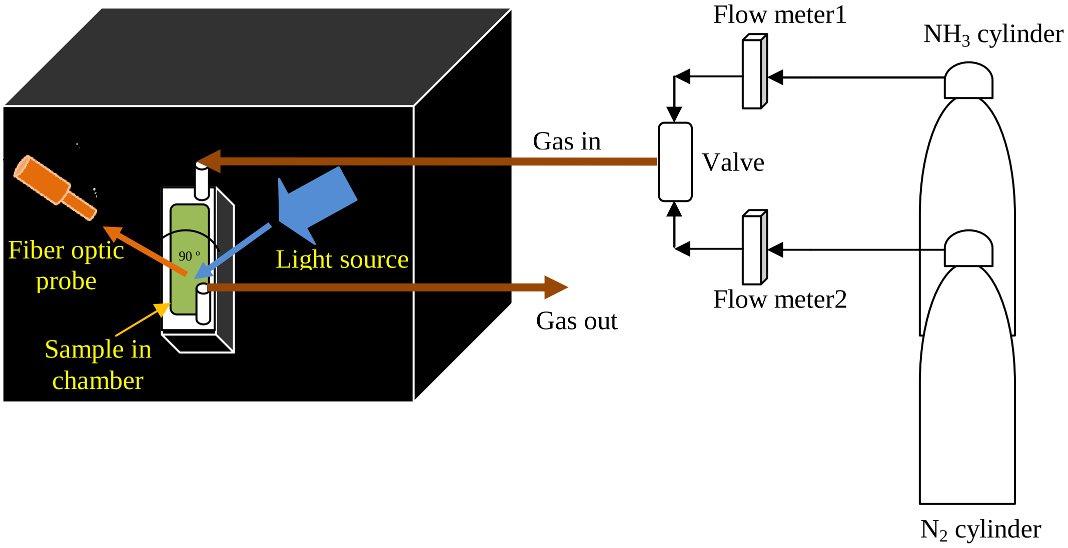

Figure 3.2 Schematic of the reflectance measurement set-up for ammonia sensing

3.3.2 Effect of solvent of PANI/PMMA solution

The solvent of polymer solution is a parameter which influences the morphology of electropun fiber and efficiency of ammonia sensing. The composition 1 of PANI/PMMA solution in Table 3.1 preparing in DMF, DMF:ethyl acetate (1:1) and ethyl acetate:acetont (1:1) were fabricated and evaluated the sensing performance. Initial percent reflectance (%R*i*), the change of percent reflectance (Δ%R) and response profile were measured.

3.3.3 Effect of PANI concentration

Various polymer blend solutions were prepared with the concentration of PANI ranging from 0.8 to 3.2% w/w (a percentage of PANI in PANI/PMMA fibers) and the PANI/PMMA composition was varied as described in Table 3.1 for all solvent systems including DMF, DMF:ethyl acetate (1:1) and ethyl acetate:acetone (1:1). The reflectance of electrospun fiber at various condition ns was measured at 1000 ppm ammonia gas exposure.

3.3.4 Response time and Recovery time

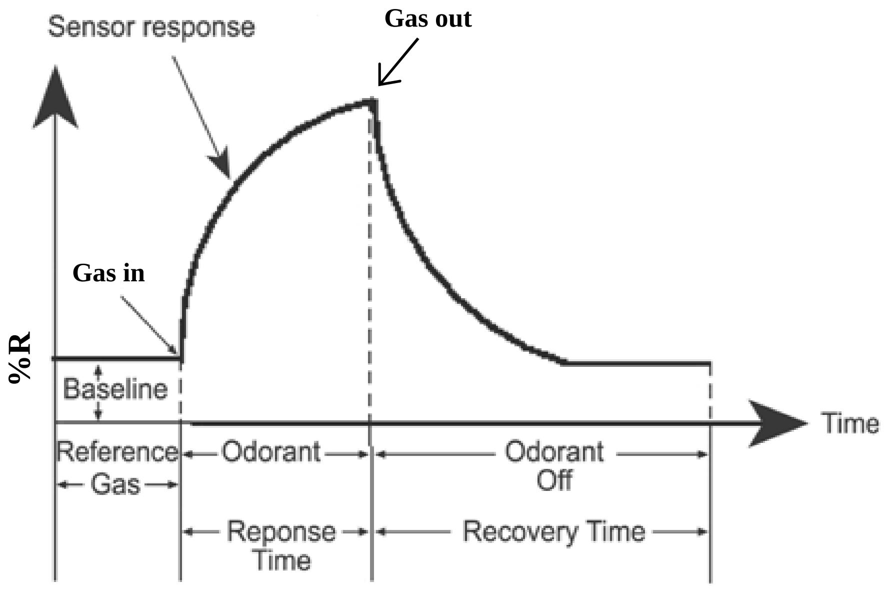

Figure 3.3 Response time and Recovery time [44]

The sensing of ammonia by an electrospun PANI/PMMA composite fibrous mats was reversible. Therefore, the change of reflectance of electrospun was measured on the exposure of ammonia gas and after turn off the gas (and purged N_2) as shown in Figure 3.3. The response time was determined as the time period from the start of ammonia gas exposure to the maximum change of the reflectance (Figure 3.3). The recovery time was determined as the time period from turning off the gas to the initial reflectance of electrospun PANI/PMMA composite fibrous mats. (Note that the reflectance of electrospun PANI/PMMA composite fibrous mats after recovery may be not equals the initial value due to efficiency of adsorption and desorption.)

CHAPTER IV

RESULTS AND DISCUSSION

4.1 Characterization of the electrospun PANI/PMMA composite fibrous mats

4.1.1 Fourier transform infrared spectrometer (FT-IR)

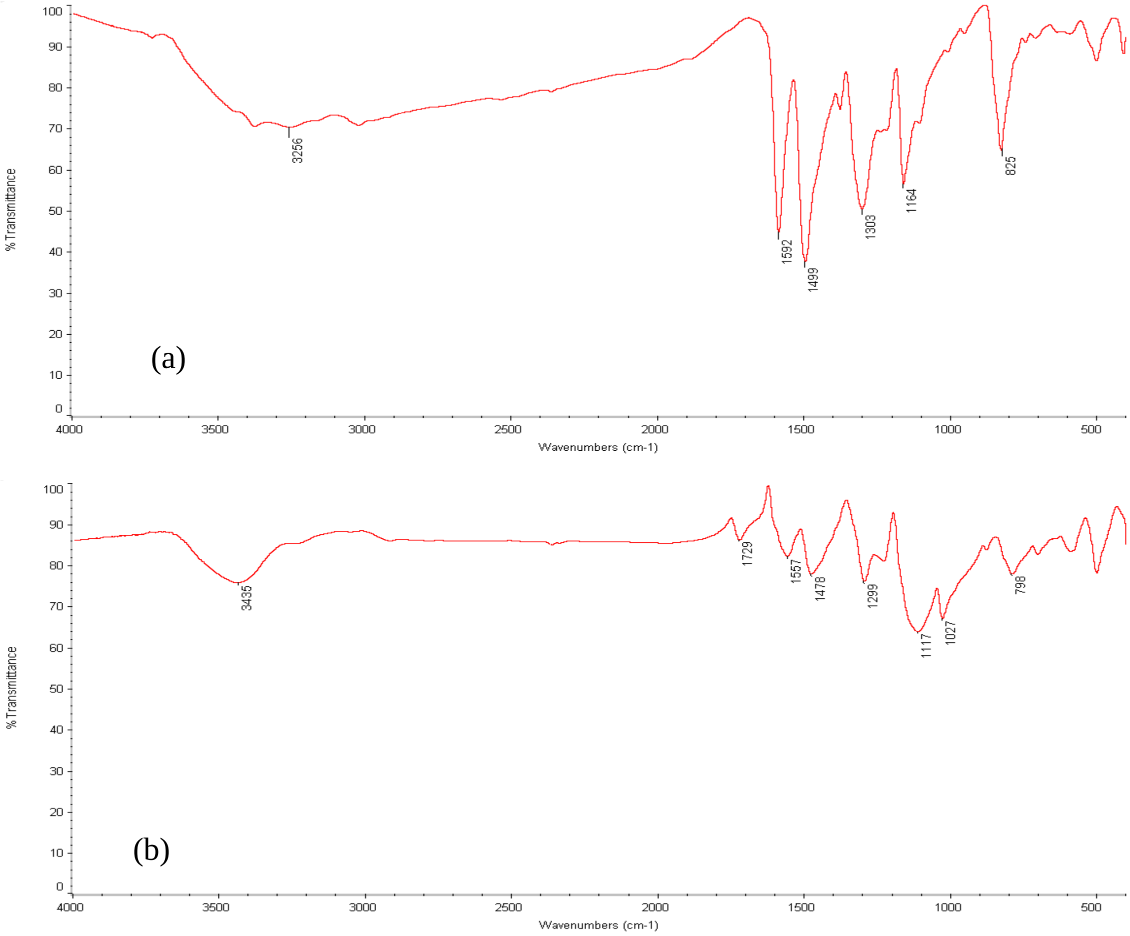

Figure 4.1 FT-IR spectra of PANI powder; (a) PANI-EB (b) PANI-ES

FT-IR analysis was used to identify the chemical structure of polyaniline (PANI). The IR spectrum of PANI in emeraldine base (PANI-EB) was shown in Figure 4.1(a) and tabulated the characteristic peaks in Table 4.1.The IR spectrum of CSA doped PANI (PANI-ES) is shown in Figure 4.1(b) and tabulated the characteristic peaks in Table 4.2.

Table 4.1 The IR characteristic peaks of PANI-EB

Wavenumber (cm^{-1})	Functional group
3256	N-H stretching of aromatic amine
1592	C=C stretching of quinoid imine
1499	C=C stretching of benzenoid diamine
1303	C-N-C stretching of a secondary of aromatic amine for both quinoid and benzenoid segments
1164	Vibration mode of quinoid ring
825	Out of plane bending of para-substitute of aromatic benzene ring

Table 4.2 The IR characteristic peaks of PANI-ES

Wavenumber (cm^{-1})	Functional group
3435	N-H stretching of aromatic amine
1729	C=O of cyclohexanone
1557, 1478	Aromatic C–C stretching vibrations
1299, 1117	Aromatic amine stretching
1027	S=O stretching of CSA doping
798	Out of plane hydrogen deformation of aromatic ring in PANI unit sequences

The observed characteristic peaks of PANI backbone are similar between PANI-EB and PANI-ES. But the PANI-ES shows C=O band of cyclohexanone at 1729 cm^{-1} because of the effect of ring strain [79]. Furthermore, the stretching band of S=O represents an absorption band at 1027 cm^{-1} confirmed the presence of sulfonic groups of CSA in PANI-ES [80]. As a result, conversion of nonconductive form of PANI (PANI-EB) to conductive form (PANI-ES) was successfully obtained.

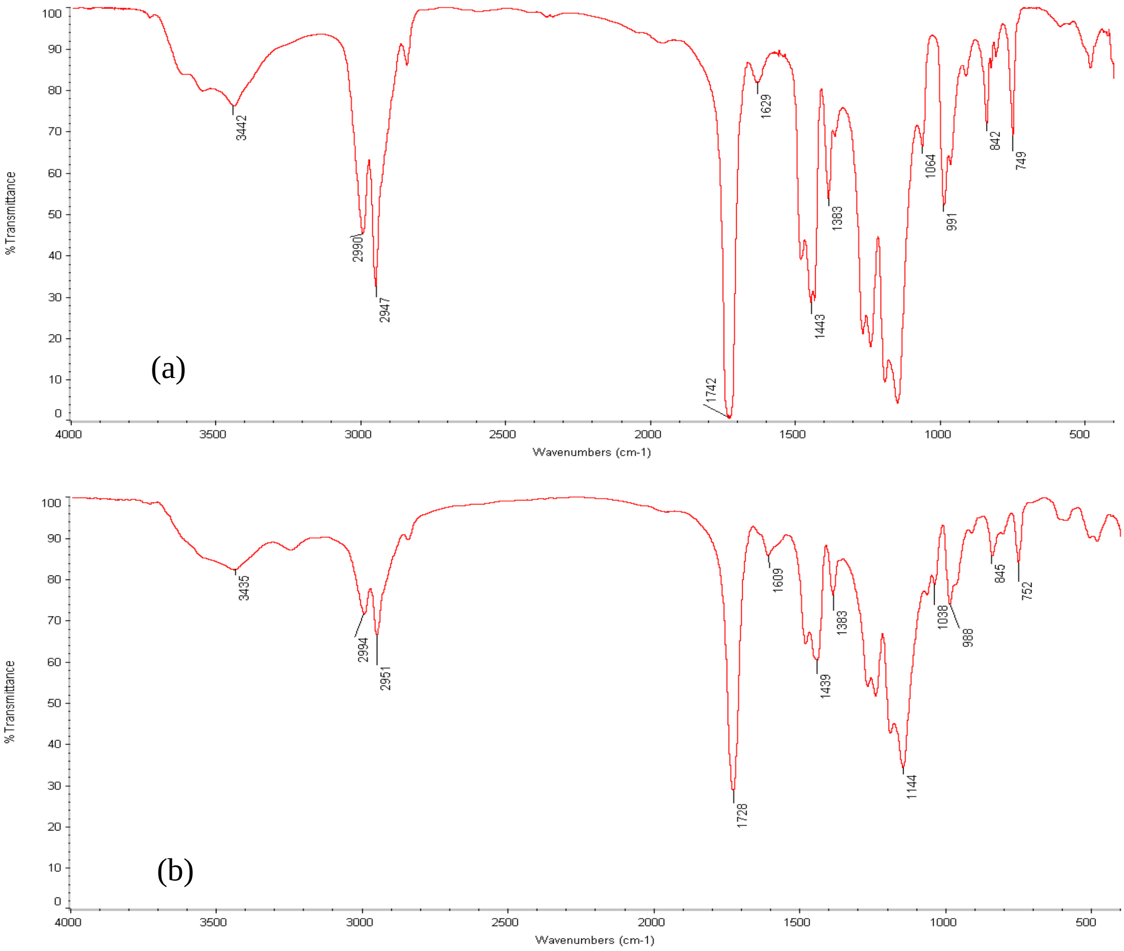

Figure 4.2 FT-IR spectra of fibers; (a) PMMA (b) CSA doped PANI blended with PMMA

Figure 4.2(a) shows the IR spectrum of PMMA fibers and tabulated the characteristic peaks in Table 4.3. The IR spectrum of CSA doped PANI blended with PMMA fibers was shown in Figure 4.2(b) and tabulated the characteristic peaks in Table 4.4.

Table 4.3 The IR characteristic peaks of PMMA fibers

Wavenumber (cm^{-1})	Functional group
2990	C–H stretching of $–CH_3$ group
2947	C–H stretching of $–CH_2$ group
1742	Acrylate carboxyl group stretching vibrations
1443	C–H bending of the $–CH_3$ group
1383, 749	α-methyl group vibrations
1150-1250	C–O–C stretching

Table 4.4 The IR characteristic peaks of CSA doped PANI blended with PMMA fibers

Wavenumber (cm^{-1})	Functional group
2994	C–H stretching of $–CH_3$ group
2951	C–H stretching of $–CH_2$ group
1728	Acrylate carboxyl group stretching vibrations
1383, 753	α-methyl group vibrations
1038	S=O stretching of CSA doping
1150-1250	C–O–C stretching

The IR spectrum of PMMA fibers showed the sharp peak intensity observed at 1742 cm^{-1} which is due to the presence of the acrylate carboxyl group stretching vibrations. The bands at 842 cm^{-1}, 991 cm^{-1} and 1064 cm^{-1} are characteristic absorption vibration of PMMA. The IR spectrum of CSA doped PANI blended with PMMA fibers showed all slightly different peaks from that of PMMA fibers. The intensity of peak is reduced when CSA doped PANI blended with PMMA such as the peak at 1742 cm^{-1} in PMMA was shifted to 1728 cm^{-1} in electrospun PANI/PMMA composite fibrous mats and increasing of intensity due to C=O stretching vibration goes on reducing [82]. The peak at 1038 cm^{-1} shows S=O stretching of CSA doping but lower intensity. Moreover, there are two peaks at ~3400 cm^{-1} and ~1600 cm^{-1} which are attributed to the –OH group stretching and bending vibrations, respectively, of physisorbed moisture [81]. The changes can be attributed to formation of hydrogen bonding between these groups due to H donation in NH group. H bonding allows compatibility between PANI and polymers containing carbonyl group and improves the formation of an inter-penetrating network of PANI and the matrix chain [83].

4.1.2 Reflection spectroscopy of PMMA, PANI-EB and PANI-ES

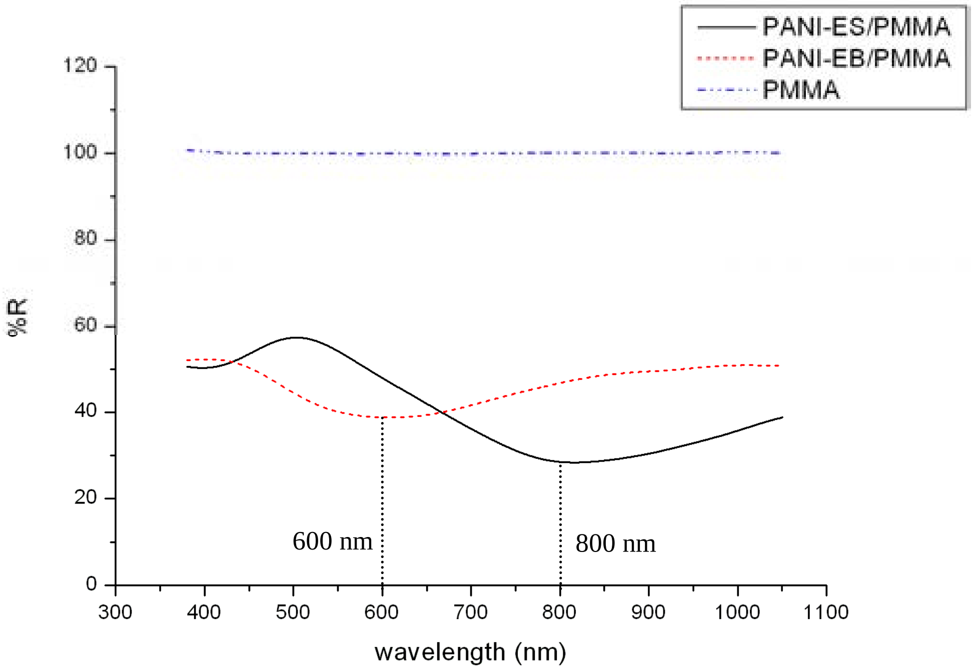

Figure 4.3 Reflection spectra of electrospun PANI-ES/PMMA and PANI-EB/PMMA composite fibers

Figure 4.3 shows the reflection spectra of electrospun fibers of PANI-ES/PMMAcomposite and PANI-EB/PMMA composite at wavelength range 400 to 1000 nm using electrospun PMMA fibrous mat as a blank to set 100%R. Generally, the conjugated polymers are often highly colored because their π-π* energy gap falls within the visible region [84]. The spectrum of PANI-EB exhibits reflectance at 600 nm due to excitation of the quinoid structure. CSA doped PANI (PANI-ES) showed clear green color with reflectance at 800 nm. They can be arised from the polaron transition in the conjugated PANI chains [85]. Jin et al. [86] developed of a polyaniline-base optical ammonia sensor. They found that PANI film treated with hydrochloric (PANI-ES) had the maximum absorbance at 800 nm and PANI-EB film had the maximum absorbance at 600 nm.

4.2 Fiber formation and morphology of the electrospun PANI/PMMA composite fibrous mats

There are many variables that affect the morphology of the electrospun fibers. The parameters can be divided into solvent in polymer solution processing condition and PANI concentration.

4.2.1 Effect of solvent in PANI/PMMA solution

Solvent system used to dissolve polymer dramatically influences on electrospinnability. The properties of solvent used in this study are summarized in Table 4.5. The key solvent properties are conductivity, surface tension, volatility and dielectric constant [65]. PMMA was dissolved in various solvents including DMF, DMF:ethyl acetate and ethyl acetate:acetone, whereas PANI was dissolved in NMP. SEM images of electrospun PMMA fibers and PANI/PMMA composite fibers were shown in Figure 4.4 and Figure 4.5, respectively.

Table 4.5 Properties of solvents; boiling point (T_b), density (ρ), viscosity (η), solubility parameter (δ), surface tension (γ), vapor pressure (P_{vap}) and dielectric constant (ε) [87, 88]

Solvent	**Chemical formula**	**T_b (^oC)**	**ρ at 25^{o}C (g/cm^3)**	**η at 25^{o}C (cP)**	**δ ($MPa^{1/2}$)**	**γ at 20 ^{o}C (mN/m)**	**P_{vap} at 20 ^{o}C (Torr)**	**ε at 25^{o}C**
NMP	C_5H_9NO	202	1.028	1.666	11	40.7^b	0.32	32.0
DMF	C_3H_7NO	153	0.9445	0.802	24.7	36.76	2.7	36.71
Ethyl acetate	$C_4H_8O_2$	77	0.9006^a	0.455^a	18.2	26.29	73.0	6.02
Acetone	C_3H_6O	56	0.7844	0.306	19.7	26.26	184.5	20.7

a= at 20 ^{o}C *b= at 25^{o}C*

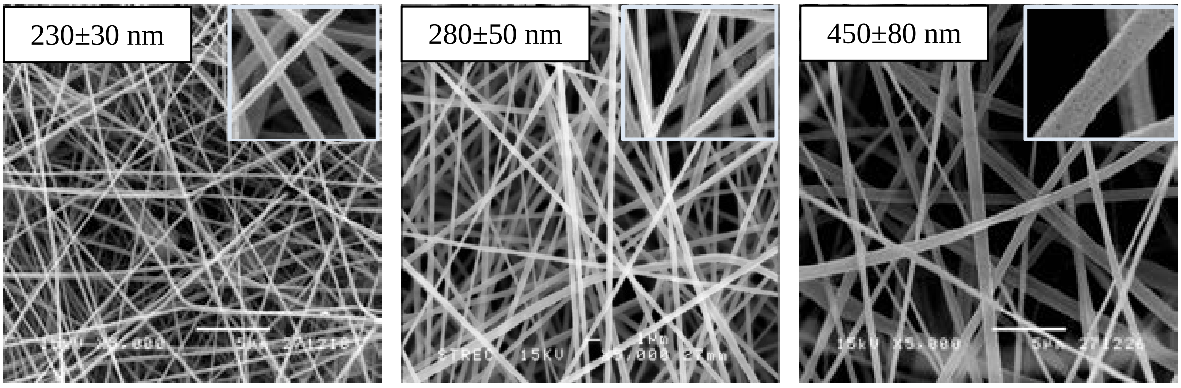

(a) (b) (c)

Figure 4.4 SEM images of electrospun PMMA fibers from PMMA solution in: (a) DMF, (b) DMF:ethyl acetate (1:1) and (c) ethyl acetate: acetone (1:1). The insets show the enlarged image. Electrospinning condition: voltage of 15 kV, flow rate at 10 μL/min and distance between the needle tip and collector of 10 cm

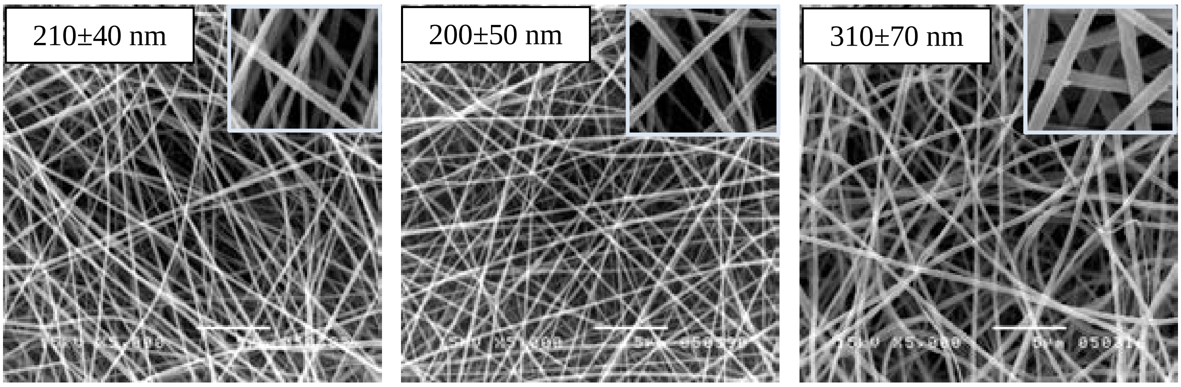

(a) (b) (c)

Figure 4.5 SEM images of electrospun PANI/PMMA composite fibers from solution in: (a) DMF, (b) DMF:ethyl acetate (1:1) and (c) ethyl acetate: acetone (1:1). The insets show the enlarged image. Electrospinning condition: voltage of 15 kV, flow rate at 10 μL/min and distance between the needle tip and collector of 10 cm

The main solvent properties which are volatility and dielectric constant were investigated.

4.2.1.1 Volatility of the solvent

Volatility of the solvent which depends on a boiling point and a vapor pressure of the solvent can attribute to the surface of fibers such as porosity. The smaller fiber diameters of electrospun result from jet extension and a minimal elongational viscosity. Essentially, the relaxation time for the polymer chains in solution needs to be matched to the rate of extensional deformation due to instability. Therefore, very rapid drying of solvent can hinder the development of small diameter of fibers. The obtained electrospun fibers from ethyl acetate: acetone had rough surface and large diameter comparing to the fibers from DMF and DMF: ethyl acetate which related to their low boiling point and high vapor pressure. Both ethyl acetate and acetone were easily evaporation during polymer solution formed jet. So this could make porous surface.

Moreover, the average diameter of electrospun PANI/PMMA fibers was smaller and more uniform than electrospun PMMA fibers. This due to the use of NMP (T_b = 202 ^{o}C) as a solvent in preparing PANI solution which slow down the drying of solvent during spinning.

4.2.1.2 Dielectric constant of the solvent

The dielectric constant of the solvent significantly influences the morphology and diameter of electrospun fibers. High dielectric constant solvents dramatically reduce both the bead formation and diameter of the fibers. The strength of the dielectric constants of the used solvents was DMF>NMP>acetone>ethyl acetate. For PMMA in ethyl acetate, no jet was ejected from the syringe. This caused by the very low dielectric constant of ethyl acetate to overcome the surface tension at the end of the needle tip. The order of diameters of obtained fibers from different solvent used were DMF<DMF:ethyl acetate<ethyl acetate:acetone which were consistent with dielectric constant of solvent. Moreover, the average diameter of electrospun PMMA fibers was larger than that of electrospun PANI/PMMA fibers because of high dielectric constant of NMP solvent in PANI solution. This reduces diameter of the fibers and improves morphology of the fibers.

4.2.2 Effect of processing parameters of electrospinning

In this part, the PANI/PMMA solution of composition 1 in Table 3.1 using DMF:ethyl acetate in PMMA solution was used to investigate an effect of processing parameters of electrospinning. The various parameters, the average diameter and fiber formation were described in Table 4.6. The average diameter range was 170-290 nm and fiber formation was all fine fibers. The detail of each parameter will discuss in next section.

Table 4.6 Fiber formation and average diameter of fibers at various processing parameters of electrospinning

flow rate (μL/min)	electric potential (kV)	distance (cm)	fiber formation	average diameter of fibers (nm) [a]
5	10	10	fine fibers	190±30
10	10	10	fine fibers	290±30
	15	7	fine fibers	230±50
		10	fine fibers	200±50
		13	fine fibers	190±70
	20	10	fine fibers	170±90

[a] diameter of fiber was averaged from 30 fibers.

4.2.2.1 Electric potential

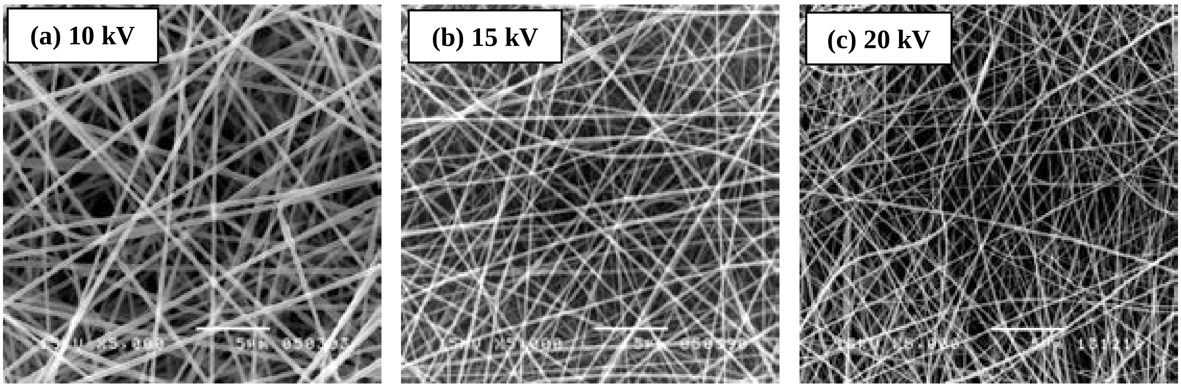

290±30 nm 200±50 nm 170±90 nm

Figure 4.6 SEM images of electrospun formed electric potential; (a) 10 kV, (b) 15 kV and (c) 20 kV. Original magnifications 5,000x (flow rate of 10 µL/min and distance between needle and collector of 10 cm)

Generally, the increasing electric potential increased mass transfer and resulted in faster rate of charged jets. As a result the diameters of fiber and bead form were decreased when used high electric potential. Figure 4.6 shows SEM images of electrospun at 10 kV, 15 kV and 20 kV (keeping other parameters constant). All of them had significant different diameter. The average diameter of electrospun fibers was decreased followed what described above when increased electric potential. At higher electric potential than 20 kV, the solution cannot fabricate fibers since the acidic solution and fast evaporation of solvent made electric spark and uneven fibers. At lower electric potential than 10 kV, the fibers also cannot fabricate due to insufficient electric potential. When compared the obtained fiber at 15 kV and 20 kV, the average diameter using 20 kV (170 nm) was smaller than using 15 kV (200 nm). However, the fiber using 15 kV was more uniform as a small standard deviation (SD) value. Thus, 15 kV of electric potential was chosen for fabricating PANI/PMMA composite fibers by the electrospinning process.

4.2.2.2 Flow rate of PANI/PMMA solution

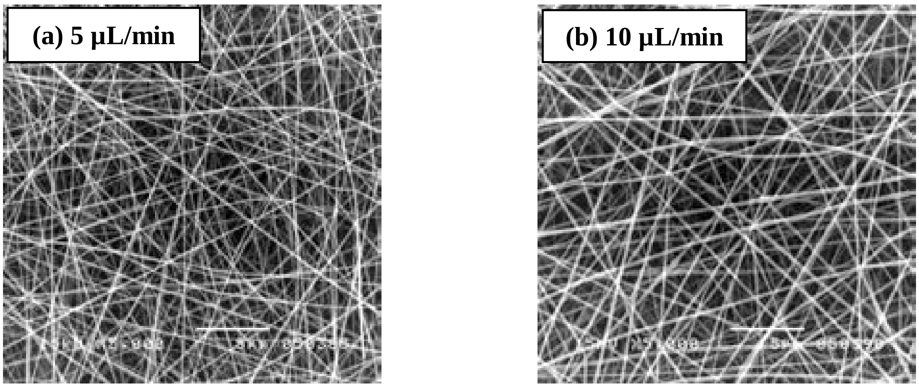

190±30 nm 200±50 nm

Figure 4.7 SEM images of electrospun formed flow rate; (a) 5 μL/min and (b) 10 μL/min. Original magnifications 5,000x (electric potential of 15 kV and distance between needle and collector of 10 cm)

Normally, the increase of flow rate will increase diameter of fibers and decrease electrostatic density. In this work two different flow rate including 10 μL/min and 15 μL/min were investigated. The morphology and the average diameter were shown in Figure 4.7. The average fiber diameters obtained from two different flow rate were not significantly different. Therefore, the flow rate was selected at 15 μL/min in order to fasten the electrospinning process.

4.2.2.3 Distance between a needle and a collector

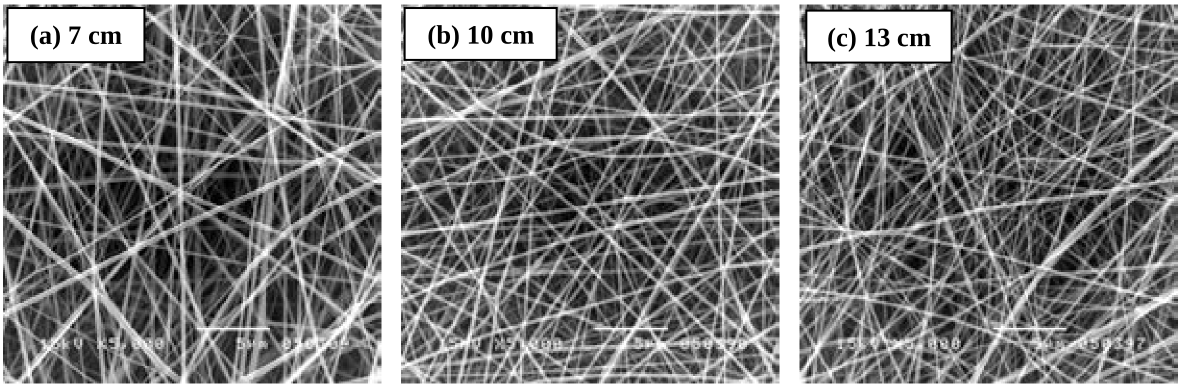

230±50 nm 200±50 nm 190±70 nm

Figure 4.8 SEM images of electrospun formed distance between a needle and collector; (a) 7 cm, (b) 10 cm and (c) 13 cm. Original magnifications 5,000x (electric potential of 15 kV and flow rate of 10 µL/min)

The distance between a needle and a collector affected diameter fibers due to evaporation time of solvent. Increasing the gap distance between a needle and a collector will reduce a fiber diameter. Three different distances were studied in this work including 7 cm, 10 cm and 13 cm. When increasing the gap distance, the average diameter was decrease which followed as discussed above. The selected gap distance was 10 cm because the morphology was fine and more uniform than that at distance of 13 cm.

Effect of processing parameters of electrospinning was found that morphology of electrospun in each various parameters did not change (fine fiber) but the average diameter was changed. Therefore, the optimum condition for processing of electrospinning was electric potential of 15 kV, flow rate of 10 µL/min and gap distance of 10 cm.

4.2.3 Effect of PANI/PMMA concentration

The solutions of 6%w/v PMMA in different solvent systems were blended with different amount of PANI to study the effect of PANI concentration. SEM images of electrospun PANI/PMMA fibers obtained from various %w/w of PANI in different solvents were shown in Figure 4.9 and the average diameters and fiber formation were summarized in Table 4.7. The obtained fibers using DMF and DMF:ethyl acetate as a solvent were smooth and fine but using ethyl acetate:acetone got rough fibers.

Table 4.7 The average diameter and fiber formation with different %PANI in each solvent system

PMMA solution in	%PANI (w/w) in PANI/PMMA fibers	Average diameter of fibers (nm) (n=30)	fiber formation
DMF	3.2	210±40	smooth fibers
	2.4	200±50	
	1.6	220±30	
	0.8	180±30	
DMF:ethyl acetate	3.2	200±50	smooth fibers
	2.4	210±40	
	1.6	220±40	
	0.8	210±50	
Ethyl acetate:acetone	3.2	310±70	rough fibers
	2.4	300±80	
	1.6	320±60	
	0.8	440±80	

From the analysis of variance (ANOVA), the fiber diameters obtained from DMF and DMF:ethyl acetate solvent systems at all %w/w PANI, except the fibers with 0.8% w/w PANI in DMF were similar and smaller than those from ethyl acetate:acetone solvent system. The average diameters of fibers were nearly 200 nm whereas those from ethyl acetate:acetone solvent system were nearly 300 nm, except the fibers with 0.8% w/w PANI (440 nm). For the fibers with 0.8% w/w PANI in DMF and ethyl acetate:acetone, their average diameters were significantly different from the others due to a volume of using solvent (Table 3.1) and solvent properties. When compared amongst solvent and effect of NMP (dissolved PANI), the fiber diameter of DMF was similar to that of DMF:ethyl acetate due to the same solvent effect of DMF and NMP which were difficult to evaporate and high dielectric constant. Both ethyl acetate and acetone evaporated easily so NMP was main effect to cause a large fiber diameter. Moreover, the fibers obtained from DMF and DMF:ethyl acetate solvent systems were more uniform than those obtained from ethyl acetate:acetone solvent system (smaller SD value). The results of ANOVA were summarized in Appendix.

.

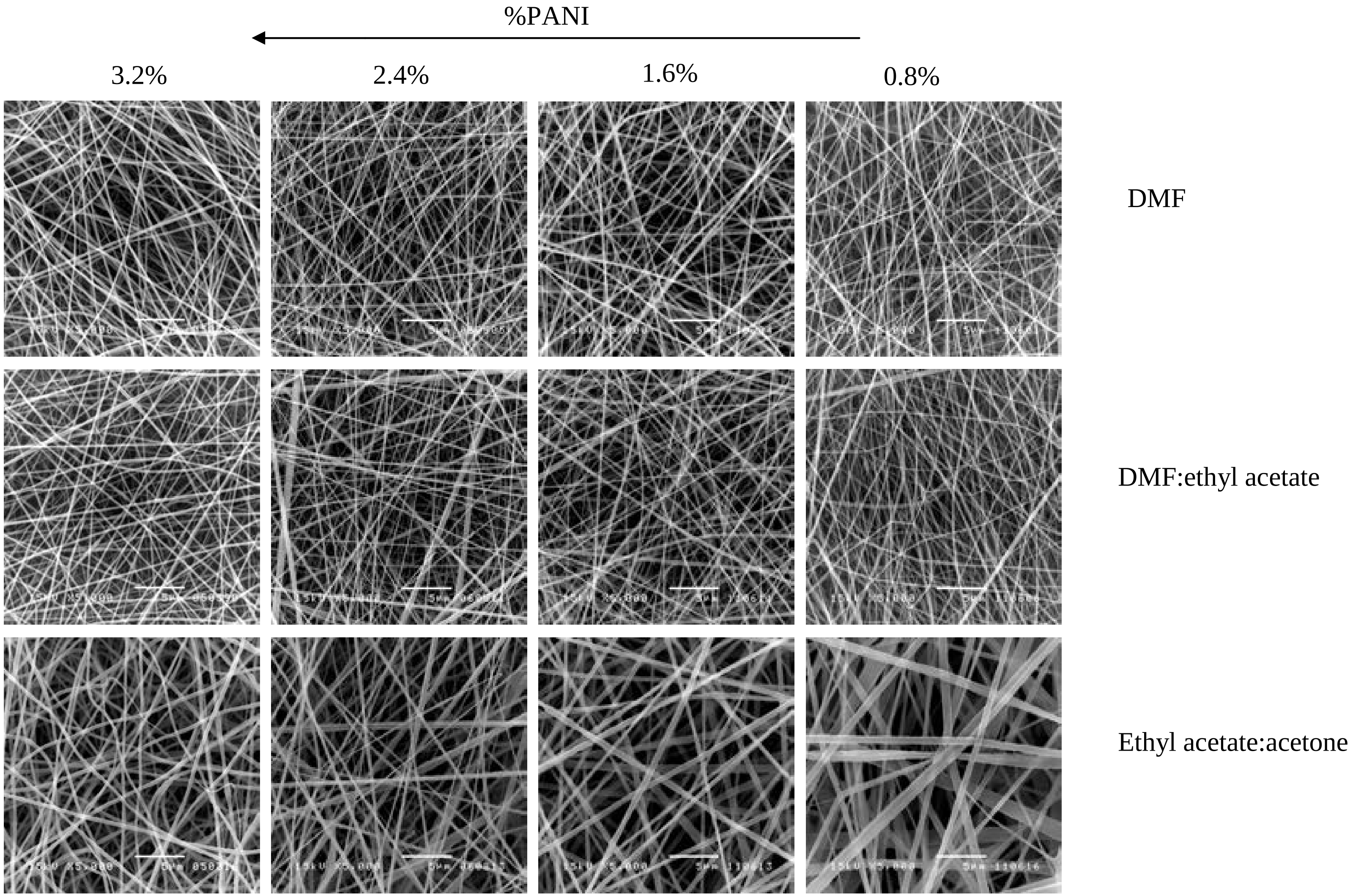

Figure 4.9 SEM images of electrospun PANI/PMMA composite fibers at different %PANI in various solvent

4.3 Ammonia sensing

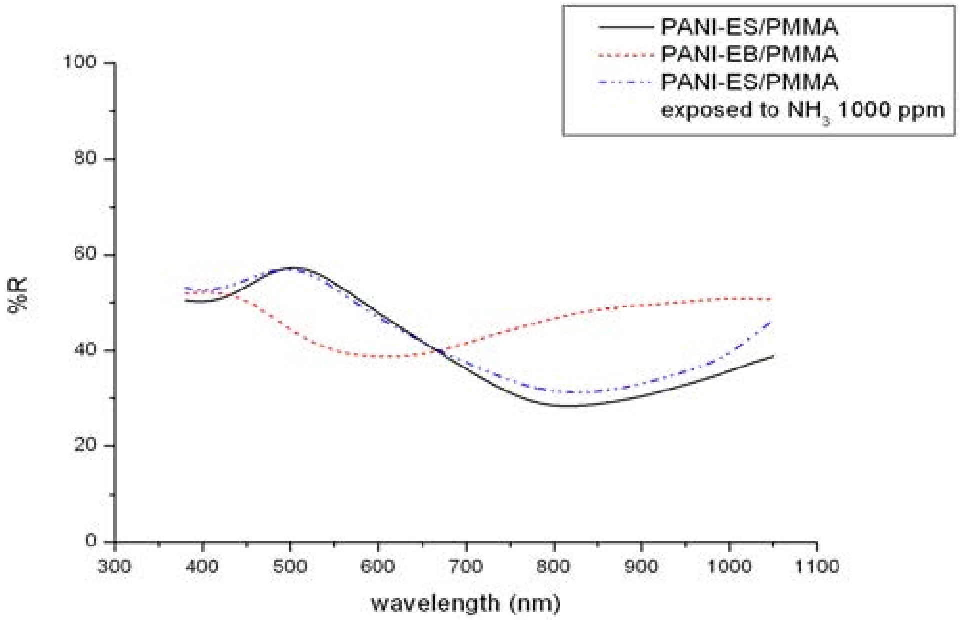

Figure 4.10 Reflection spectra of electrospun PANI-ES/PMMA, PANI-EB/PMMA and PANI-ES/PMMA composite fibers exposed to 1000 ppm ammonia gas

As mention in section 4.1.2, the reflection spectra of PANI-EB and PANI-ES were different and can be distinctly distinguished at wavelength about 600 nm (PANI-EB absorption) and 800 nm (PANI-ES absorption). Figure 4.10 showed the reflection spectra of electrospun PANI/PMMA composite fibrous mats before and after the exposure of 1000 ppm NH_3 gas. The decrease of reflectance at 600 nm as the generation of PANI-EB was not clearly seen. This might be caused by the amount of PANI-ES changed to PANI-EB after exposure to 1000 ppm ammonia gas was small comparing to original PANI-ES in electrospun PANI/PMMA mats. However, the increase of reflectance at 800 nm as the loss of PANI-ES can be observed. The patterns of reflection spectra in various solvent systems were similar. Therefore, the reflectance at 800 nm was measured for the study of ammonia gas sensing by electrospun PANI/PMMA composite fibrous mats.

4.3.1 Effect of solvent of PANI/PMMA solution

Since the solvent influences the morphology of electrospun fiber (as discuss in section 4.2.1), the initial percent reflectance (%R*i*) of electrospun PANI/PMMA composite fibrous mats obtained from the three solvent systems including DMF, DMF:ethyl acetate (ratio 1:1), and ethyl acetate:acetone (ratio 1:1) were studied. As a result, %R*i* of electrospun PANI/PMMA composite fibrous mats obtained from studied solvent systems were different and order as DMF<DMF:ethyl acetate<ethyl acetate:acetone (Table 4.8). This related to the amount of PANI in the obtained fibers as PANI can dissolve and disperse well in NMP and DMF comparing to ethyl acetate and acetone. This agreed with the appearance of the prepared fibers which the most greenish noticed when using DMF as solvent.

Table 4.8 Ammonia sensing of the electrospun PANI/PMMA composite fibrous mats in various solvent systems

	PANI/PMMA fibers[a]		
	DMF	**DMF:ethyl acetate**	**ethyl acetate:acetone**
%R*i*	31.067	47.113	57.677
Δ%R	0.970	1.152	1.264
Fiber diameter (nm)	210±40	200±50	310±70
Fiber surface	smooth	smooth	rough

[a]3.2% w/w of PANI blended with 96.8% w/w of PMMA

The Δ%R values order is DMF<DMF:ethyl acetate< ethyl acetate:acetone at the same %PANI. The reason for this was the difference in fiber morphology. The morphology of the fiber prepared in DMF and DMF:ethylacetate was small and smooth but having pores or rough surface in ethyl acetate:acetone system. The rough surface and porous fiber increased the surface area of fibers and thus result the higher change of %R.

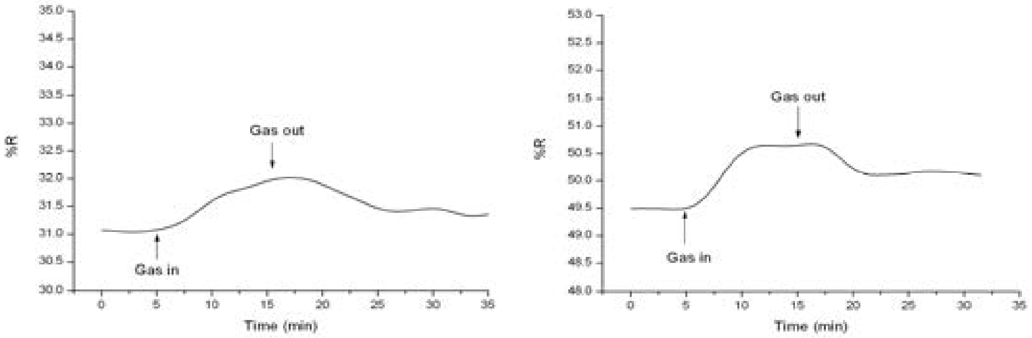

(a) DMF (b) DMF:ethyl acetate

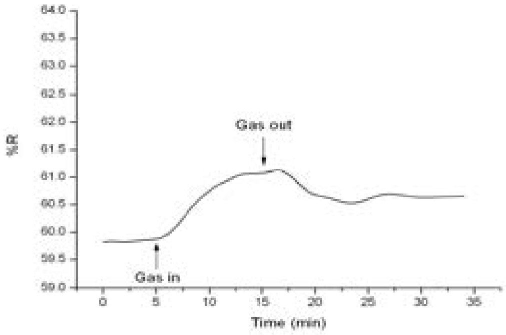

(c) ethyl acetate:acetone

Figure 4.11 Response profiles of electrospun PANI/PMMA composite fibrous mats obtained from different solvent; (a) DMF (b) DMF:ethyl acetate and (c) ethyl acetate:acetone (exposed to 1000 ppm of ammonia gas and recovery by purging with N_2 gas)

Table 4.9 Response time and recovery time in each solvent system

	DMF	**DMF:ethyl acetate**	**ethyl acetate:acetone**
Response time (min)	12.5	7.5	10.0
Recovery time (min)	10.0	7.5	10.0

The response time of electrospun fibers was the time period that turned on ammonia gas and exposed to fibers until %R of the electrospun fibers stopped changing. The recovery time was the time period that allowed the %R of the electrospun fiber returning to an initial value after turned off the ammonia gas. From Table 4.9, the electrospun PANI/PMMA composite fibrous mats in DMF:ethyl acetate gave the shortest response time at 7.5 min and could see obviously threshold. When turned off ammonia gas and purged with N_2 gas (at a minute of 15), recovery time of DMF:ethyl acetate was faster than DMF and ethyl acetate:acetone.

4.3.2 Effect of PANI concentration

PANI concentration influences both %R*i* and Δ%R. In the same solvent, the %R*i* increased when PANI concentration was decreased as shown in Table 4.10 and Figure 4.12. It could be explained that the more PANI concentration, the more apparent of green color of fiber. This could lead to less reflection. Otherwise, the less PANI concentration resulted in light green to white color of obtained fiber which was more reflection so the %R*i* was higher.

Table 4.10 %R*i* of PANI/PMMA composite fibrous mats with different %PANI and solvent systems

%w/w PANI	**%R*i***		
	DMF	**DMF:ethyl acetate**	**ethyl acetate:acetone**
3.2	31.067	47.113	57.677
2.4	39.812	51.837	69.407
1.6	55.002	56.065	71.055
0.8	65.216	77.863	87.297

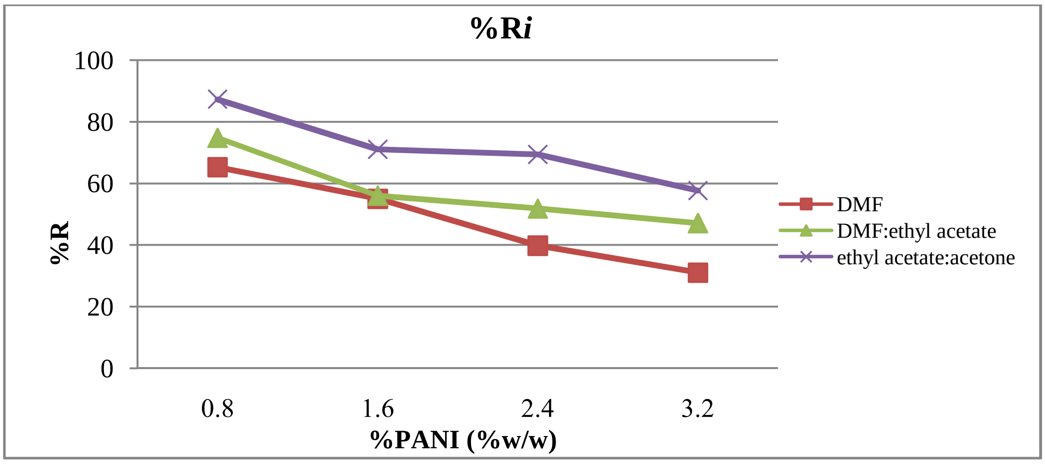

Figure 4.12 %R*i* of PANI/PMMA composite fibrous mats with different %PANI and solvent systems

Table 4.11 Δ%R of PANI/PMMA composite fibrous mats with different %PANI and solvent systems

%w/w PANI	**Δ%R**		
	DMF	**DMF:ethyl acetate**	**ethyl acetate:acetone**
3.2	0.970	1.152	1.264
2.4	1.269	1.390	1.444
1.6	1.407	1.585	1.623
0.8	1.565	1.718	1.896

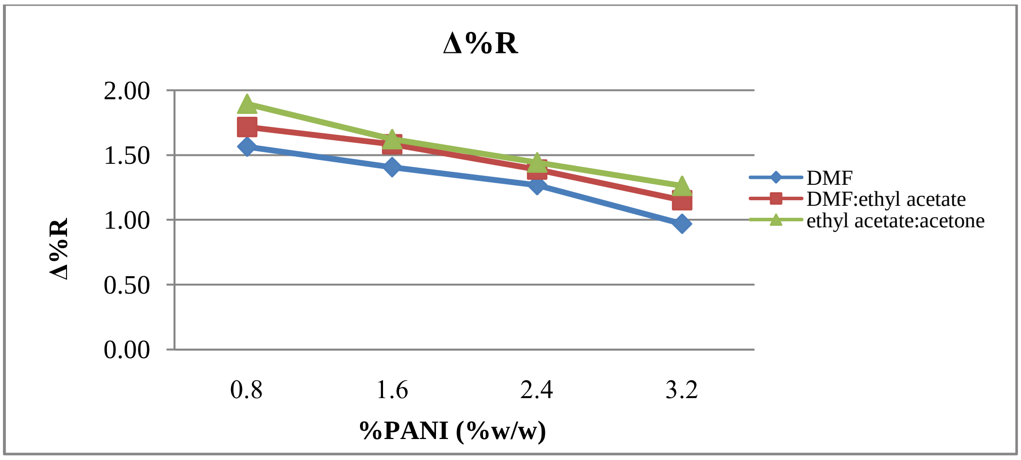

Figure 4.13 Δ%R of PANI/PMMA composite fibrous mats with different %PANI and solvent systems

From Table 4.11 and Figure 4.13, in the same solvent, Δ%R increased when PANI concentration was decreased. Highly PANI concentration could make less in the change of %R. Figure 4.14 showed the response of electrospun PANI/PMMA composite fibrous mats formed using DMF:ethyl acetate with PANI in various concentration. The response profile of 3.2, 2.4 and 1.6% w/w PANI were similar and not affected by %PANI.

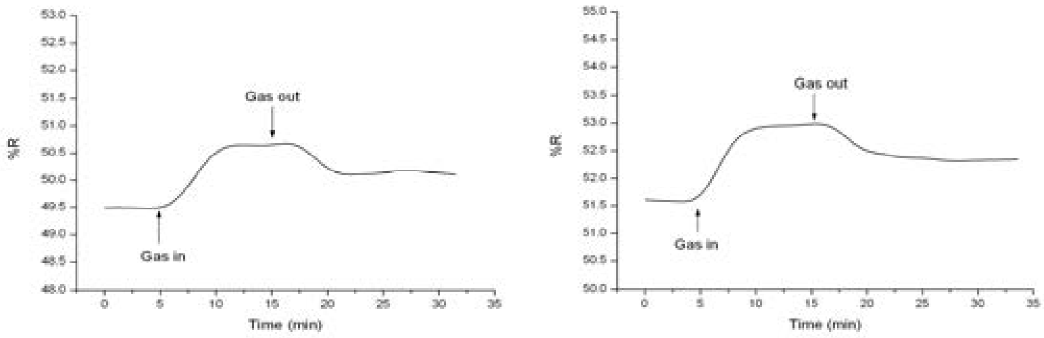

(a) 3.2% (b) 2.4%

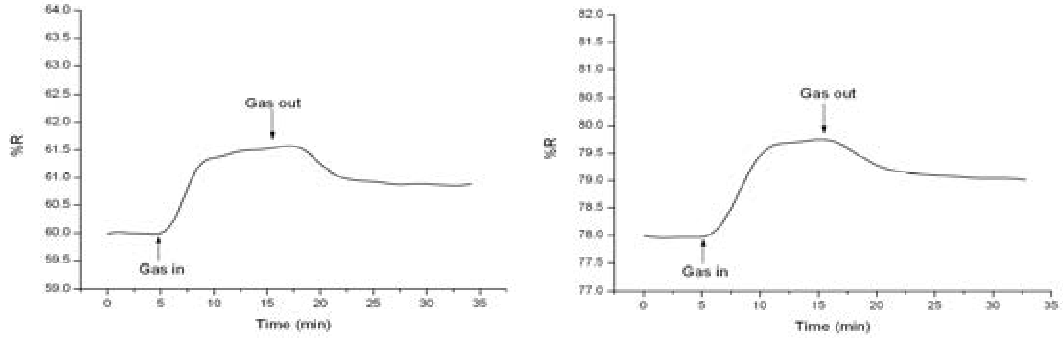

(c) 1.6% (d) 0.8%

Figure 4.14 Response profiles of electrospun formed using DMF:ethyl acetate as solvent with different %w/w PANI; (a) 3.2, (b) 2.4, (c) 1.6 and (d) 0.8 when exposed to 1000 ppm of ammonia gas

Table 4.12 Response time and recovery time in each %PANI

	3.2%	**2.4%**	**1.6%**	**0.8%**
Response time (min)	7.5	7.5	7.5	7.5
Recovery time (min)	7.5	7.5	7.5	7.5

The response time and the recovery time of all %PANI were similar as shown in Figure 4.14 and Table 4.12. The result of the reversed %R was not equal the initial %R due to chemical interaction of ammonia molecules with the electrospun PANI/PMMA composite fibrous mats might occur. Chemically adsorbed ammonia molecules had a strong interaction with the electrospun PANI/PMMA composite fibrous mats and could not be desorbed by refreshing with N_2 gas, thus the %R could not return to the initial value.

CHAPTER V

CONCLUSION

5.1 Conclusion

Polyaniline/poly(methyl methacrylate) (PANI/PMMA) composite fibrous mats had been successfully fabricated by electrospinning process with diameters ranged from 170-450 nm with the fine and smooth morphology. Fourier transform infrared spectrometer (FT-IR) used to characterize the functional group of PANI-EB, PANI-ES, PMMA and PANI/PMMA fibers. In addition, the characterizations of PANI-ES/PMMA and PANI-EB/PMMA composites fibrous mats were investigated by reflection spectroscopy. The reflection spectra indicated the clearly different between PANI-EB (high absorption at 600 nm) and PANI-ES (high absorption at 800 nm). The morphology of electrospun fibers were characterized by scanning electron microscope (SEM). The morphology and the diameter of the fibers were affected by the electric potential, the distance between a needle and a collector, the flow rate of the solution, PANI concentration and particularly solvent system. Increasing the electric potential and the distance between a needle and a collector, the fiber diameter decreased whereas the flow rate of the solution increased, the size of the fiber increased. Furthermore, the solvent system influenced the morphology and diameter due to the solvent properties which are volatility and dielectric constant. The porous surface was achieved when using the high volatility solvents. In addition, the high dielectric constant of the solvent not only reduced the bead formation but also decreased the fiber diameter. The optimum condition for electrospinning was electric potential of 15 kV, flow rate of 10 µL/min and distance between a needle and a collector of 10 cm. In this work, PANI concentration hardly affected the morphology of fibers. At 1.6, 2.4 and 3.2 %w/w of PANI in the same solvent system, the morphology and fiber diameter were not significantly different as proved by analysis of variance (ANOVA).

PANI/PMMA composite fibrous mats can use as ammonia sensing. The decrease of reflectance at 600 nm caused by the generation of PANI-EB or the increase of reflectance at 800 nm caused by the loss of PANI-ES was monitored. As exposed the PANI/PMMA composite fibrous mats to 1000 ppm of ammonia gas, the percent of reflectance at 800 nm was clearly changed and used to evaluate the ammonia gas sensing performance. The reflectance change at 600 nm was small and not suitable to determine the ammonia sensing. The sensing performance of PANI/PMMA composite fibrous mats was depended on prepared solvent and %PANI. The initial percent reflectance (%R*i*) as well as the change of percent reflectance (Δ%R) of PANI/PMMA composite fibrous mats prepared from different solvent systems were increased as a series; DMF<DMF:ethyl acetate<ethyl acetate:acetone. This behavior was related to the morphology of obtained fibers and solubility of PANI in the solvents. For effect of %PANI, when %PANI in the fibers increase %R*i* and Δ%R was decreased. For the response time and the recovery time, PANI/PMMA composite fibrous mats using DMF:ethyl acetate solvent system gave the best sensing profile and the fastest sensing in which the response time was 7.5 min and recovery time was 7.5 min.

We have successfully prepared the PANI/PMMA composite fibrous mats via electrospinning process for using as ammonia sensing. The new sensor is stable, reversible, low cost, fast response, and easy to regenerate which is suitable for the preliminary detection.

5.2 Suggestion of future work

The limitation of ammonia sensing was the lower amount of PANI due to limited by its solubility. The humidity surrounding a sensor will be influent the ammonia detection capability of electrospun PANI/PMMA composite fibrous mats. Therefore, humidity is a parameter that must be dealt within the process of sensor developing. The limitation of PANI in solvent systems due to solvent properties and solubility of PANI affected sensing performance of fibers. Thus, adding more PANI can improve sensing performance electrospun PANI/PMMA composite fibrous mats. Many parameters can affect the diameter and morphology of fiber especially solvent system.

Therefore, these parameters will be investigated during electrospinning process development. Additionally, the proposed sensor should be developed to detect at low concentration of ammonia gas.

REFERENCES

[1] Timmer, B., Olthuis, Olthuis, W. and Berg, A.V.D. Ammonia sensors and their applications-a review. Sensors and Actuators B 107 (2005): 666-677.

[2] Ding, B., Yamazaki, M. and Shiratori, S. Electrospun fibrous polyacrylic acid membrane-based gas sensors. Sensors and Actuators B 106 (2005): 477-483.

[3] Prasad, G.K., Radhakrishnan, T.P., S., K.D. and Krishna, M.G. Ammonia sensing characteristics of thin film based on polyelectrolyte templated polyaniline. Sensors and Actuators B 106 (2005): 626-631.

[4] Zakrzewska, K. Mixed oxides as gas sensors. Thin Solid Films 391 (2001): 229-238.

[5] Sberveglieri, G. Recent developments in semiconducting thin-film gas sensors. Sensors and Actuators B 23 (1995): 103-109.

[6] Imawan, C., Imawan, C., Solzbacher, F., Steffes, H. and Obermeier, E. Gas-sensing characteristics of modified-MoO_3 thin films using Ti-overlayers for NH_3 gas sensors. Sensors and Actuators B 64 (2000): 193-197.

[7] Varghese, O., Kichambre, P., Gong, D., Ong, K., Dickey, E. and Grimes, C. Gas sensing characteristics of multi-wall carbon nanotubes. Sensors and Actuators B 81 (2001): 32-41.

[8] Lukaszewicz, J. Carbon materials for chemical sensors: a review. Sensor Letters 4 (2006): 53-98.

[9] Lonergan, M., Severin, E., Doleman, B., Beaber, S., Grubb, R. and Lewis, N. Array-based vapor sensing using chemically sensitive, carbon black-polymer resistor. Chemistry of Materials 8 (1996): 2298-2312.

[10] Unde, S., Ganu, J. and Radhakrishnan, S. Conducting polymer-based chemical sensor: characteristics and evaluation of polyaniline composite films. Advanced Functional Materials 6 (1996): 151-157.

[11] Bai, H. and Shi, G. Gas sensors based on conducting polymers. Sensors 7 (2007): 267-307.

[12] Nicho, M.E., Trejo, M., García-Valenzuela, A., Saniger, J.M., Palacios, J. and Hu, H. Polyaniline composite coatings interrogated by a nulling optical-transmittance bridge for sensing low concentrations of ammonia gas. Sensors and Actuators B 76 (2001): 18-24.

[13] Yuan, J., El-Sherif, M.A., MacDiarmid, A.G. and Jones, W.E. Fiber optic chemical sensors using a modified conducting polymer cladding. In Proceedings of SPIE, The International Society for Optical Engineering. 2001.

[14] El-Dib, I.F., Sayed, M.W., Ahmed, M.S. and Elkodary, M. Synthesis of polyaniline nanostructures in micellar solutions. Journal of Applied Polymer Science 124 (2012): 3200-3207.

[15] Matsuguchi, M., Io, J., Sugiyama, G. and Sakai, Y. Effect of NH_3 gas on the electrical conductivity of polyaniline blend films. Synthetic Metals 128 (2002): 15-19.

[16] Renker, D.H. and Chun, I. Nanometre diameter fibres of polymer produced by electrospinning. Nanotechnology 7 (1996): 216-223.

[17] Jagadeesh, B.V., Satheesh, K.K., Trivedi, D.C., Murthy, V.R. and Natarajan, T.S. Electrical properties of electrospun fibers of PANI-PMMA composites. Journal of Engineered Fibers and Fabrics 2 (2007): 25-31.

[18] Bai, H., Zhao, L., Lu, C., Li, C. and Shi, G. Composite nanofibers of conducting polymers and hydrophobic insulating polymers: Preparation and sensing applications. Polymer 50 (2009): 3292-3301.

[19] Catargiu, A.M. and Grigoraş, M. Polyaniline synthesis in the presence of three macrocyclic compounds. Acta Chemica Iasi 19 (2011): 81-100.

[20] Yoon, C.O., Reghu, M., Moses, D., Cao, Y. and Heeger, A.J. Transports in blends of conducting polymers. Synthetic Metals 69 (1995): 255-258.

[21] Fraysse, J., Planés, J., Dufresne, A. and Guermache, A. Thermomechanical studies of polyaniline/poly(methyl methacrylate) blends: Relationship with conducting properties. Macromolecules 34 (2001): 8143-8148.

[22] Desai, K. and Sung, C. DOE optimization and phase morphology of electrospun nanofibers of PANI/PMMA blends. NSTI-Nanotech 4 (2004): 429-432.

[23] Tomar, A.K., Mahendia, S., Chahal, R.P. and Kumar, S. Structural and dielectric spectroscopic studies of polyaniline-poly(methyl methacrylate) composite films. Synthetic Metals 162 (2012): 820-826.

[24] Li, D., Huang, J. and Kaner, R.B. Polyaniline nanofibers: A unique polymer nanostructure for versatile applications. Accounts of Chemical Research 42 (2009): 135-145.

[25] Yilmaz, F. Polyaniline: synthesis, characterization, solution properties and composites. Doctoral dissertation, Department of Polymer Science and Technology, The Graduate School of Natural and Applied Sciences of Middle east technical University, 2007.

[26] Hao, Q. Development of conductometric polymer sensor for gaseous hydrogen chloride. Doctoral dissertation, Faculty of Chemistry and Pharmacy, University of Regensburg, 2003.

[27] Stejskal, J., Sapurina, I., Proke, J. and Zemek, J. In-situ polymerized polyaniline films. Synthetic Metals 105 (1999): 195-202.

[28] Kolla, H.S., Surwade, S.P., Zhang, X., Macdiarmid, A.G. and Manohar, S.K. Absolute molecular weight of polyaniline. Journal of the American Chemical Society 127 (2005): 16770 - 16771.

[29] Babu, V.J., Kumar, V.S.P., Subha, G.J., Kumari, V., Natarajan, T.S.N., A. S. and Ramakrishna, S. AC Conductivity studies on PMMA-PANI (HCl) nanocomposite fibers produced by electrospinning. Journal of Engineered Fibers and Fabrics 6 (2011): 54-59.

[30] Du, Z., Li, C., Li, L., Yu, H., Wang, Y. and Wang, T. Ammonia gas detection based on polyaniline nanofibers coated on interdigitated array electrodes. Journal of Materials Science: Materials in Electronics 22 (2011): 1857-1861.

[31] Jeevananda, T. and Siddaramaiah. Synthesis and characterization of polyaniline filled PU/PMMA interpenetrating polymer networks. European Polymer Journal 39 (2003): 569-578.

[32] Malinauskas, A. Chemical deposition of conducting polymers. Polymer 42 (2001): 3957-3972.

[33] Wang, Y., Jing, X. and Kong, J. Polyaniline nanofibers prepared with hydrogen peroxide as oxidant. Synthetic Metals 157 (2007): 269-275.

[34] Zhang, L., Wan, M. and Y., W. Nanoscaled polyaniline fibers prepared by ferric chloride as an oxidant. Macromolecular Rapid Communications 27 (2006): 366-371.

[35] Ayad, M.M., Amer, W.A. and Whdan, M. Polyaniline film formation using ferric chloride as an oxidant. Journal of Applied Polymer Science 125 (2012): 2695-2700.

[36] Ayad, M.M. and Whdan, M. The effect of HCl on the polymerization of aniline with ferric chloride. Colloid Journal 70 (2008): 549-554.

[37] Ansari, A.A., Khan, R., Sood, K.N. and Malhotra, B.D. Polyaniline-cerium oxide nanocomposite for hydrogen peroxide sensor. Journal of Nanoscience & Nanotechnology 9 (2009): 4679-4685.

[38] Omastová, M., Mosnáčková, K., Trchová, M., Konyushenko, E.N., Stejskal, J., Fedorko, P. and Prokeš, J. Polypyrrole and polyaniline prepared with cerium(IV) sulfate oxidant. Synthetic Metals 160 (2010): 701-707.

[39] Gonzalez, I., Munoz, M.E., Santamaria, A., Pomposo, J.A., Grande, H. and Rodriguez- Parra, J. Highly conducting polyaniline gels. Macromolecular Rapid Communications 23 (2002): 659-663.

[40] Syed, A.A. and Dinesan, M.K. Review: Polyaniline-A novel polymeric material. Talanta 38 (1991): 815-37.

[41] Sengupta, P.P. and Adhikari, B. Influence of polymerization condition on the electrical conductivity and gas sensing properties of polyaniline. Material Science and Engineering A 459 (2007): 278-285.

[42] Abrantes, L.M., Correia, J.P., Savic, M. and Jin, G. Structural modifications during conducting polymer formation-an ellipsometric study. Electrochimica Acta 46 (2001): 3181-3187.

[43] Bhadra, S., Khastgir, D., Singha, N.K. and Lee, J.H. Progress in preparation, processing and applications of polyaniline. Progress in Polymer Science 34 (2009): 783-810.

[44] Sawatruksa, C. Polyaniline blended with polyvinyl alcohol for ammonia sensing. Master’s thesis, Department of Chemistry, Faculty of Science, Chulalongkorn University, 2006.

[45] Ram, M.K., Mascetti, G., Paddeu, S., Maccioni, E. and Nicolini, C. Optical, structural and fluorescence microscopic studies on reduced form of polyaniline: The leucoemeraldine base. Synthetic Metals 89 (1997): 63-69.

[46] Heeger, A.J. Semiconducting and metallic polymers: the fourth generation of polymeric materials. Synthetic Metals 125 (2002): 23-42.

[47] Kukla, A.L., Shirshor, Y.M. and Piletsky, S.A. Ammonia sensors based on sensitive polyaniline films. Sensors and Actuators B 37 (1996): 135-140.

[48] Wallace, G.G., Spinks, G.M., Kane-Maguire, L.A.P. and Teasdale, P.R. Conductive Electroactive Polymers. Boca Raton, FL: CRC Press Taylor & Francis Group, 2009.

[49] Wan, M. and Yang, J. Studies on the structure and electrical properties of poly(*ortho*-toluidine). Synthetic Metals 73 (1995): 201-204.

[50] Athawale, A.A., Kulkarni, M.V. and Chabukswar, V.V. Studies on chemically synthesized soluble acrylic acid doped polyaniline. Materials Chemistry and Physics 73 (2002): 106-110.

[51] Hu, H., Saniger, J.M. and Banuelos, J.G. Thin films of polyaniline-polyacrylic acid composite by chemical bath deposition. Thin Solid Films 347 (1999): 241-247.

[52] Ryu, K.S., Moon, B.W., Joo, J. and Chang, S.H. Characterization of highly conducting lithium salt doped polyaniline films prepared from polymer solution. Polymer 42 (2001): 9355-9360.

[53] Yang, C. and Chen, C. Synthesis, characterization and properties of polyanilines containing transition metal ions. Synthetic Metals 153 (2005): 133-136.

[54] Krutovertsev, S.A., Sorokin, S.I., Zorin, A.V., Letuchy, Y.A. and Antonova, O.Y. Polymer film-based sensors for ammonia detection. Sensors and Actuators B 7 (1992): 492-494.

[55] Kukla, A.L., Shirshov, Y.M. and Piletsky, S.A. Ammonia sensors based on sensitive polyaniline films. Sensors and Actuators B 37 (1996): 135-140.

[56] Agbor, N.E., Petty, M.C. and Monkman, A.P. Polyaniline thin films for gas sensing. Sensors and Actuators B 28 (1995): 173-179.

[57] Agbor, N.E., Cresswell, J.P., Petty, M.C. and Monkman, A.P. An optical gas sensor based on polyaniline Langmuir-Blodgett films. Sensors and Actuators B 41 (1997): 137-141.

[58] Airoudja, A., Debarnota, D., Bêchec, B. and Poncin-Epaillarda, F. Development of an optical ammonia sensor based on polyaniline/epoxy resin (SU-8) composite. Talanta 77 (2009): 1590-1596.

[59] Mendelson, Y. The Biomedical Engineering Handbook. Boca Raton, FL: CRC Press LLC, 2000.

[60] Gazda, D.B. Development of colorimetric solid phase extraction (C-SPE) for in-flight monitoring of spacecraft water supplies. Doctoral dissertation, Department of Chemistry, Faculty of Science, Iowa State University, 2004.

[61] Orel, Z.C., Gunde, M.K. and Orel, B. Application of the Kubelka-Munktheory for the determination of the optical properties of solar absorbing paints. Progress in Organic Coatings 30 (1997): 59-66.

[62] Kim, J.S. and Reneker, D.H. Polybenzimidazole Nanofiber Produced by Electrospinning. Polymer Engineering and Science 39 (1999): 849-854.

[63] Bhardwaj, N. and Kundu, S.C. Electrospinning: A fascinating fiber fabrication technique. Biotechnology Advances 28 (2010): 325-347.

[64] Baji, A., Mai, Y.W., Wong, S.C., Abtahi, M. and Chen, P. Electrospinning of polymer nanofibers: Effects on oriented morphology, structures and tensile properties. Composites Science and Technology 70 (2010): 703-718.

[65] Andrady, A.L. Science and Technology of Polymer Nanofibers. New Jersey: John Wiley & Sons, Inc., 2008.

[66] Ramakrishna, S., Fujihara, K., Teo, W.E., Lim, T.C. and Ma, Z. An Introduction to Electrospinning and Nanofibers. Singapore: World Scientific Publishing Co. Pte. Ltd., 2005.

[67] Deitzel, J.M., Kleinmeyer, J., Harris, D. and Beck Tan, N.C. The effect of processing variables on the morphology of electrospun nanofibers and textiles. Polymer 42 (2001): 261-272.

[68] Afifi, A.M., Yamane, H. and Kimura, Y. Effect of polymer molecular weight on the electrospinning of polylactides in entangled and aligned fiber forms. Sen'i Gakkaishi 66 (2010): 35-42.

[69] Hohman, M.M., Shin, M., Rutledge, G. and Brenner, M.P. Electrospinning and electrically forced jets. I. Stability theory. Physics of Fluids 13 (2001): 2201-2220.

[70] Hohman, M.M., Shin, M., Rutledge, G. and Brenner, M.P. Electrospinning and electrically forced jets. II. Applications. Physics of Fluids 13 (2001): 2221-2236.

[71] Fong, H., Chun, I.D. and Reneker, H. Beaded nanofibers formed during electrospinning. Polymer 40 (1999): 4585-4592.

[72] Lee, K.H., Kim, H.Y., Khil, M.S., Ra, Y.M. and Lee, D.R. Characterization of nano-structured poly(1-caprolactone) nonwoven mats via electrospinning. Polymer 44 (2003): 1287-1294.

[73] Shawon, J. and Sung, C.M. Electrospinning of polycarbonate nanofibers with solvent mixtures THF and DMF. Journal of Materials Science 39 (2004): 4605-4613.

[74] Dong, H., Nyame, V., Macdiarmid, A.G. and Jones, W.E. Polyaniline/poly(methyl methacrylate) coaxial fibers: The fabrication and effects of the solution properties on the morphology of electrospun core fibers. Journal of Polymer Science: Part B: Polymer Physics 42 (2004): 3934-3942.

[75] Chowdhury, M. and Stylios, G. Effect of experimental parameters on the morphology of electrospun Nylon 6 fibres. IJBAS: International Journal of Basic & Applied Sciences 10 (2012): 116-131.

[76] Mo, X.M., Xu, C.Y., Kotaki, M. and Ramakrishna, S. Electrospun P(LLACL) nanofiber: a biomimetic extracellular matrix for smooth muscle cell and endothelial cell proliferation. Biomaterials 25 (2004): 1883-1890.

[77] Rodoplu, D. and Mutlu, M. Effects of electrospinning setup and process parameters on nanofiber morphology intended for the modification of quartz crystal microbalance surfaces. Journal of Engineered Fibers and Fabrics 7 (2012): 118-123.

[78] Chen, M.J. Development and parametric studies of carbon nanotube dispersion using electrospraying. Master’s Thesis, Department of Industrial and Manufacturing Engineering, FAMU-FSU College of Engineering, The Florida State University, 2007.

[79] Lee, W.J., Kim, Y.J. and Kaang, S. Electrical properties of polyanilinersulfonated polycarbonate blends. Synthetic Metals 113 (2000): 237-243.

[80] Verma, D. and Dutta, V. Role of novel microstructure of polyaniline-CSA thin film in ammonia sensing at room temperature. Sensors and Actuators B 134 (2008): 373-376.

[81] Duan, G., Zhang, C., Li, A., Yang, X., Lu, L. and Wang, X. Preparation and characterization of mesoporous zirconia made by using a poly(methyl methacrylate) template. Nanoscale Research Letters 3 (2008): 118-122.

[82] Yadav, J.B., Puri, R.K. and Puri, V. Improvement in mechanical and optical properties of vapour chopped vacuum evaporated PANI/PMMA composite thin film. Applied Surface Science 254 (2007): 1382-1388.

[83] Tomar, A.K., Mahendia, S. and Kumar, S. Structural characterization of PMMA blended with chemically synthesized PAni. Advances in Applied Science Research 2 (2011): 327-333.

[84] Sengupta, P.P., Barik, S. and Adhikari, B. Polyaniline as a gas sensor material. Materials and Manufacturing Processes 21 (2006): 263-270.

[85] Jayakannan, M., Anilkumar, P. and Sanju, A. Synthesis and characterization of new azobenzenesulfonic acids doped conducting polyaniline. European Polymer Journal 42 (2006): 2623-2631.

[86] Jin, Z., Su, Y. and Duan, Y. Development of a polyaniline-based optical ammonia sensor. Sensors and Actuators B 72 (2001): 75-79.

[87] Dean, J.A. Lange’s Handbook of Chemistry. Singapore: McGRAW-HILL, 1999.

[88] Smallwood, I.M. Handbook of Organic Solvent Properties. New York: John Wiley&Son Inc., 1996.

APPENDIX

Analysis of variance (ANOVA)

The analysis of variance (ANOVA) compares between the means of two or more samples. The significantly different can evaluate from F-value and P-value. If F-value is greater than F critical or P-value is less than or equal to 0.05, the null hypothesis is reject.

Table A-1 ANOVA test of PANI/PMMA fibers diameter of all %w/w PANI in DMF

ANOVA: Single Factor
SUMMARY

Groups	*Count*	*Sum*	*Average*	*Variance*
3.2% w/w PANI	30	6.20	0.206667	0.00134
2.4% w/w PANI	30	5.87	0.195667	0.002267
1.6% w/w PANI	30	6.59	0.219667	0.000796
0.8% w/w PANI	30	5.46	0.182	0.001223

ANOVA

Source of Variation	*SS*	*df*	*MS*	*F*	*P-value*	*F crit*
Between Groups	0.0231	3	0.0077	5.47371	0.001488	2.682809
Within Groups	0.16318	116	0.001407			
Total	0.18628	119				

The diameter of fibers from 3.2%, 2.4%, 1.6% and 0.8% w/w PANI are significantly different.

Table A-2 ANOVA test of PANI/PMMA fibers diameter of 3.2%, 2.4% and 1.6% w/w PANI in DMF

ANOVA: Single Factor
SUMMARY

Groups	*Count*	*Sum*	*Average*	*Variance*
3.2% w/w PANI	30	6.20	0.206667	0.00134
2.4% w/w PANI	30	5.87	0.195667	0.002267
1.6% w/w PANI	30	6.59	0.219667	0.000796

ANOVA

Source of Variation	*SS*	*df*	*MS*	*F*	*P-value*	*F crit*
Between Groups	0.00866	2	0.00433	2.949961	0.0576	3.101296
Within Groups	0.1277	87	0.001468			
Total	0.13636	89				

The diameter of fibers from 3.2%, 2.4% and 1.6% w/w PANI are not significantly different.

Table A-3 ANOVA test of PANI/PMMA fibers diameter of all %w/w PANI in DMF:ethyl acetate

ANOVA: Single Factor

SUMMARY

Groups	*Count*	*Sum*	*Average*	*Variance*
3.2% w/w PANI	30	5.89	0.196333	0.002431
2.4% w/w PANI	30	6.20	0.206667	0.00134
1.6% w/w PANI	30	6.47	0.215667	0.001681
0.8% w/w PANI	30	6.39	0.213	0.002436

ANOVA

Source of Variation	*SS*	*df*	*MS*	*F*	*P-value*	*F crit*
Between Groups	0.006649	3	0.002216	1.124038	0.342351	2.682809
Within Groups	0.22873	116	0.001972			
Total	0.235379	119				

The diameter of fibers from 3.2%, 2.4%, 1.6% and 0.8% w/w PANI are not significantly different.

Table A-4 ANOVA test of PANI/PMMA fibers diameter of all %w/w PANI in ethyl acetate:acetone

Anova: Single Factor

SUMMARY

Groups	*Count*	*Sum*	*Average*	*Variance*
3.2% w/w PANI	30	9.45	0.315	0.004433
2.4% w/w PANI	30	8.88	0.296	0.007004
1.6% w/w PANI	30	9.62	0.320667	0.003965
0.8% w/w PANI	30	13.08	0.436	0.006487

ANOVA

Source of Variation	*SS*	*df*	*MS*	*F*	*P-value*	*F crit*
Between Groups	0.364083	3	0.121361	22.17765	2.02E-11	2.682809
Within Groups	0.634777	116	0.005472			
Total	0.998859	119				

The diameter of fibers from 3.2%, 2.4%, 1.6% and 0.8% w/w PANI are significantly different.

Table A-5 ANOVA test of PANI/PMMA fibers diameter of 3.2%, 2.4% and 1.6% w/w PANI in ethyl acetate:acetone

ANOVA: Single Factor

SUMMARY

Groups	*Count*	*Sum*	*Average*	*Variance*
3.2% w/w PANI	30	9.45	0.315	0.004433
2.4% w/w PANI	30	8.88	0.296	0.007004
1.6% w/w PANI	30	9.62	0.320667	0.003965

ANOVA

Source of Variation	*SS*	*df*	*MS*	*F*	*P-value*	*F crit*
Between Groups	0.010016	2	0.005008	0.975417	0.38112	3.101296
Within Groups	0.446657	87	0.005134			
Total	0.456672	89				

The diameter of fibers from 3.2%, 2.4% and 1.6% w/w PANI are not significantly different.

VITA

Miss Piriya Khwanphrom was born on May 7, 1987 in Bangkok, Thailand. She graduated with a Bachelor of Science degree in Chulalongkorn University in 2009. After that, she has been a graduated student at Program of Petrochemistry and Polymer Science, Faculty of Science, Chulalongkorn University and become a member of Chromatography and Separation Research Unit. She finished her Master's degree of Science in 2012.

Poster presentation and proceeding

"Effect of solvent on the morphology of polyaniline/poly(methyl methacrylate) composite fibers prepared by electrospinning" Piriya Khwanphrom, Puttaruksa Varanusupakul. Poster presentation and proceeding, *Pure and Applied Chemistry International Conference 2012 (PACCON 2012),* The Empress Hotel, Chiang Mai, Thailand, 11-13 January, 2012.